DISSERTATION

SMALL RNA METHYLATION IN CAENORHABDITIS ELEGANS

Submitted by

Joshua Svendsen

Graduate Degree Program in Cell and Molecular Biology

In partial fulfillment of the requirements

For the Degree of Doctor of Philosophy

Colorado State University

Fort Collins, Colorado

Spring 2020

Doctoral Committee:

Advisor: Taiowa A. Montgomery

Carol J. Wilusz
Erin Osborne Nishimura
Thomas J. LaRocca

ABSTRACT

SMALL RNA METHYLATION IN CAENORHABDITIS ELEGANS

Eukaryotes employ small RNAs and RNA interference (RNAi) for such diverse tasks as regulating gene expression, suppressing viral infections, and defending their genomes from foreign or parasitic sequences such as pseudogenes or transposons. In the germlines of animals, piwi-interacting RNAs (piRNAs) target and silence sequences such as these to ensure that genetic information passes from one generation to the next intact. For many animals, piRNAs must be methylated at their 3' ends to protect them from degradation, and loss of stable piRNAs results in sterility. In this study, we identify a role for piRNA methylation in maintaining germline integrity in *C. elegans*. We also show that methylation is important for piRNA stability in worm embryos but dispensable in the adult germline. Further, we identify additional classes of methylated small RNAs: exogenous primary short interfering RNAs (siRNAs) and a subpopulation of micro RNAs (miRNAs), as well as characterizing factors that influence which small RNAs are methylated. Finally, we provide a brief review of recent advances in the field of piRNA biology that detail the rules governing piRNA targeting and a means by which endogenous *C. elegans* genes avoid silencing by the piRNA-dependent RNAi pathway.

ACKNOWLEDGEMENTS

There is no hyperbole in saying, nor shame in admitting, that I would not have finished this project without a robust support network. I cannot name everyone who helped me, but I can say with certainty that I, and anyone who benefits from this research, owe a debt of gratitude to the following people:

My fiancé Annie Walker, for her constant support, superhuman patience, and unwavering confidence in me.

My parents Dana and Leah Svendsen, my siblings Matt and Maggie Svendsen, my soon-to-be in-laws Barb and Jim Walker, and my grandparents Virg and Shari Menning, Darrell Svendsen, Janelle and Bob Marx, and Ione Svendsen, for helping me keep perspective and remember what's important.

My advisor Tai Montgomery, for guiding the project from start to finish and for patiently training me into something resembling a competent scientist.

My advisory committee members Carol Wilusz, Erin Nishimura, Olve Peersen, and Tom LaRocca, for providing insightful feedback on my work and guiding my development as a researcher.

My labmates Brooke Montgomery, Kristen Brown, Kailee Reed, Rachel Tucci, Taylor Marks, Tarah Vijayasarathy, and Kora Kastengren, for providing experimental assistance, moral support, hilarious conversations, sage advice, impromptu therapy, and an inexhaustible supply of goofy shenanigans, each in varying proportion.

My close friends Chris Bondy, Tom and Talia Bickett (and my unofficial nephews PJ and

Finn), Jared Ribstein, Ali Blake, Josh Leopold, and Erin Hinson, for giving me something other than worms to think about, supporting my creative endeavors, and nodding along to my weird rants.

Justin Lee and Marylee Layton, for processing dozens of my sequencing samples and generally being kind and pleasant folks.

My fellow CMB students both past and present, for providing a supportive and positive research community.

And finally, all others that I did not mention by name, but who nonetheless contributed to my success.

TABLE OF CONTENTS

CHAPTER 1: Introduction

RNA interference. RNA interference (RNAi) is a conserved gene regulatory process in which noncoding RNAs called small RNAs serve as sequence-specific guides for Argonaute effector proteins to influence diverse cellular processes. First identified in the 1990s (Lee et al., 1993; Wightman et al., 1993), RNAi has since been found to regulate developmental timing, maintenance of genome and germline integrity, environmental response, and tuning of coding gene expression. Nearly all eukaryotes employ RNAi for some or all of these functions (Ketting, 2011; Claycomb, 2014).

Argonaute proteins are central to the molecular mechanism of RNAi. These proteins form an RNA-induced silencing complex (RISC) by binding small RNAs and using them as sequence-specific guides to identify and engage mRNA targets (Figure 1.1). When bound to Argonaute proteins, the 5’ end of the small RNA is seated in the mid domain, while the 3’ end is bound to the paz domain (Kuhn and Joshua-Tor 2013). Between these domains is the piwi domain, which contains the catalytic domain of the protein, often referred to as the slicer domain. The slicer domain is required for the function of some, but not all, Argonaute proteins (Tolia and Joshua-Tor 2007). In general, Argonaute proteins downregulate mRNA targets identified by their small RNA guides. The specific means of this downregulation varies, and may be initiated by cleaving the mRNA (catalyzed by the slicer domain), recruiting decay factors to it, or otherwise repressing translation (Ketting, 2011; Ameres and Zamore, 2013; Claycomb, 2014).

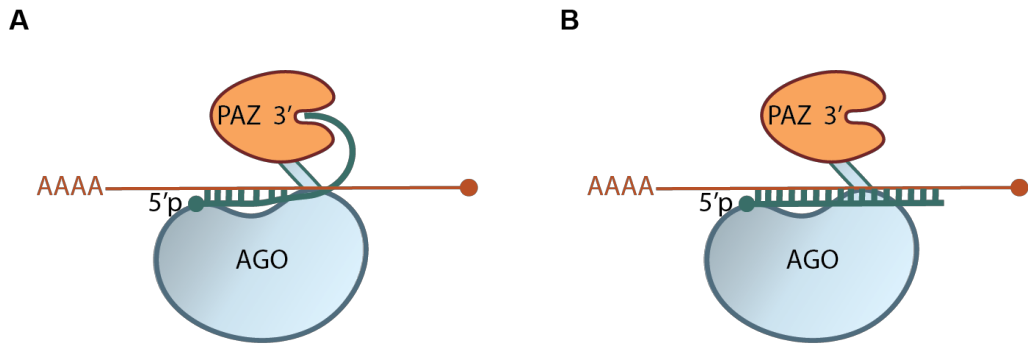

Figure 1.1. Argonaute structure and small RNA target engagement. (A) A small RNA seated in an Argonaute engaging a target with imperfect pairing. (B) A small RNA seated in an Argonaute engaging a target with perfect pairing. Adapted from Kuhn and Joshua-Tor, 2013 with information from Horwich et al. 2007 incorporated.

Small RNAs. There are three known classes of small RNAs, classified by their biogenesis pathways and molecular features: microRNAs (miRNAs), small interfering RNAs (siRNAs), and piwi interacting RNAs (piRNAs).

miRNAs. miRNA precursors are transcribed by RNA polymerase II in the nucleus and contain short hairpin foldbacks, often with bulges resulting from imperfect pairing in the hairpin stem (Lee et al., 2004; Bartel, 2004). These hairpins are cleaved from the longer transcript by the endonuclease Drosha before being exported to the cytoplasm, where they are further processed into a miRNA duplex by Dicer. This duplex is loaded into an Argonaute protein, where one strand remains bound while the other is dissociated, either to be degraded or bound by another Argonaute protein (Figure 1.2) (Bartel, 2004; Ameres and Zamore, 2013).

Like other classes of small RNAs, miRNAs serve as sequence-specific guides to recruit Argonaute effectors to mRNA targets for downregulation. miRNAs rely on partial sequence complementarity, guided by a “seed region” at positions 2-10, to identify their targets. These seed sequences are shared among different miRNAs within the same “family,” and can be conserved across species (Bartel, 2009). In addition to pairing in the 5’ seed region, miRNAs also contain supplementary base pairing regions nearer the 3’ end of the RNA (Wee et al., 2012). miRNAs guide their associated Argonaute protein to the 3’ UTR of a target mRNA, where they use endonucleolytic cleavage, mRNA destabilization, or translational repression to downregulate their targets and control diverse biological pathways (Bartel, 2004; Ameres and Zamore, 2013).

siRNAs. Canonical siRNAs are derived from double-stranded RNA (dsRNA) that undergoes cleavage by Dicer into to a short duplex with 2 nt overhangs. After binding to

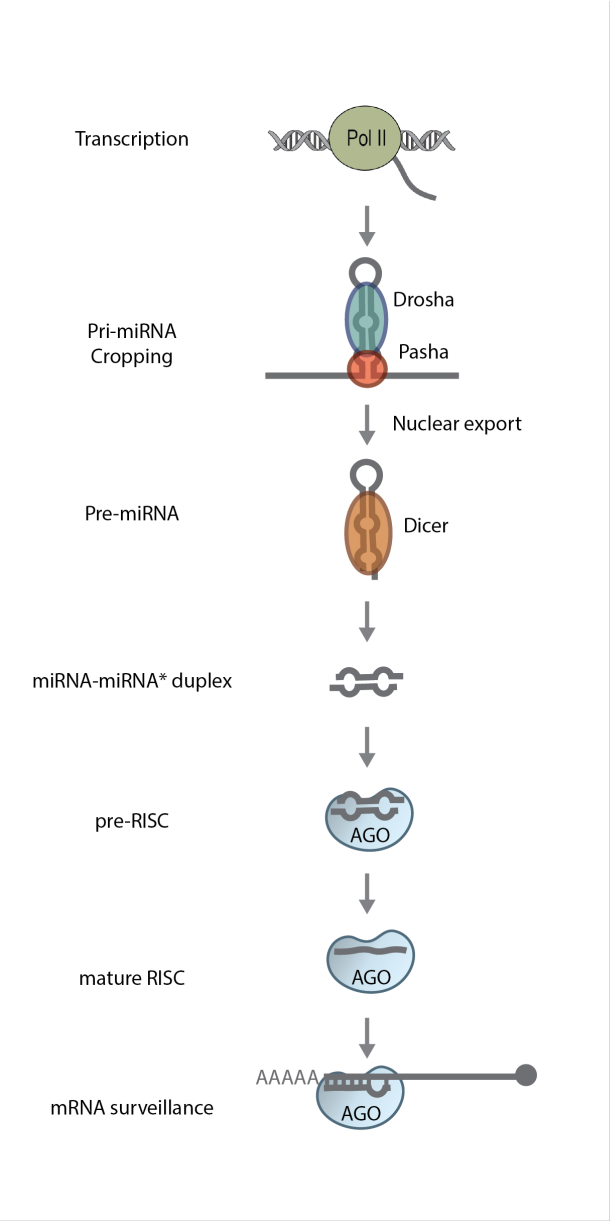

Figure 1.2. miRNA biogenesis. The miRNA pathway from transcription to mRNA engagement. Both the canonical pathway (left) and an alternative pathway (right) are depicted. From Ameres and Zamore, 2013.

an Argonaute protein, one strand is discarded while the other is used as a guide for identifying mRNA targets (Bernstein et al., 2001; Tomari and Zamore, 2005; Carthew and Sontheimer, 2009). The sources of these double-stranded precursors vary, with mice and flies generating them via bidirectional transcription from a single locus, hybridization of complementary transcripts from individual loci, or hairpins derived from transcription of inverted repeats (Claycomb, 2014). siRNAs typically interact with their targets with perfect complementarity to perform various functions such as regulation of coding genes, defense of the genome against transposons, and innate immune response to viral infection (Carthew and Sontheimer, 2009; Claycomb, 2014). In a research context, dsRNA can be introduced into a cell, allowing its siRNA processing machinery to produce siRNAs and effect targeted knockdown of complementary mRNA (Mello and Conte, 2004). In *C. elegans*, exogenous dsRNA taken up from the environment is processed by Dicer into an siRNA duplex, loaded into the Argonaute RDE-1, and matured into a functional RNA induced silencing complex (RISC) that initiates silencing of complementary RNA via the Mutator-dependent RNAi pathway (detailed in “RNAi in *C. elegans*” section) (Tabara et al., 2002; Pak and Fire, 2007; Sijen et al., 2007).

Endogenous siRNAs in *C. elegans* fall into several categories, identified by their length, 5’ nucleotide, and the Argonaute protein with which they associate. 26G-RNAs, named for their 26 nucleotide length and 5’ guanidine residue, associate with the Argonaute proteins ALG-3, ALG-4, and ERGO-1 (Han et al., 2009). Those that bind ALG-3 and -4 form a distinct class and are primarily known for their participation in the spermatogenesis pathway (Conine et al., 2010). ERGO-1 class 26G-RNAs are

expressed from embryogenesis through the early larval stages and establish an RNAi-mediated gene regulation program that targets pseudogenes, replicated genes, and persists through adulthood (Vasale et al., 2010; Fisher et al. 2011). To produce these 26G-RNAs, target mRNAs are engaged by a protein complex containing the RNA-dependent RNA polymerase RdRP RRF-3, which generates dsRNA substrate for Dicer by synthesizing a complementary strand of RNA (Han et al., 2009; Gent et al., 2010). The resulting siRNA duplexes can then be bound by an Argonaute protein and matured to form a RISC capable of performing RNA surveillance (Figure 1.3).

In addition to 26G-RNAs, *C. elegans* also uses RdRPs to manufacture another class of siRNAs called 22G-RNAs. These small RNAs can also be further subdivided based on the Argonautes to which they bind, and they differ from canonical siRNAs in both their biogenesis and structure (Gu et al., 2009). Instead of being processed from dsRNA by Dicer, WAGO class 22G-RNAs are produced by a group of proteins called the Mutator complex, which contains numerous RNA modifying enzymes and the RdRP RRF-1 (Aoki et al., 2007; Phillips et al., 2012). Although the specific mechanics of this reaction are not known, current evidence suggests that mRNA targets identified by primary small RNAs are routed into the pathway and modified into a substrate for the RdRP, which then produces secondary 22G-RNAs antisense to the target (Ambros et al., 2003; Aoki et al., 2007; Pak and Fire 2007; Sijen et al., 2007; Gu et al., 2009) (For more information on primary and secondary small RNAs, see the “RNAi in *C. elegans*” section below). Structurally, these small RNAs have a triphosphate group at their 5’ end rather than the monophosphate found on Dicer products (Gu et al., 2009). WAGO class 22G-RNAs are also capable of maintaining a “memory” of genes to be silenced - after a

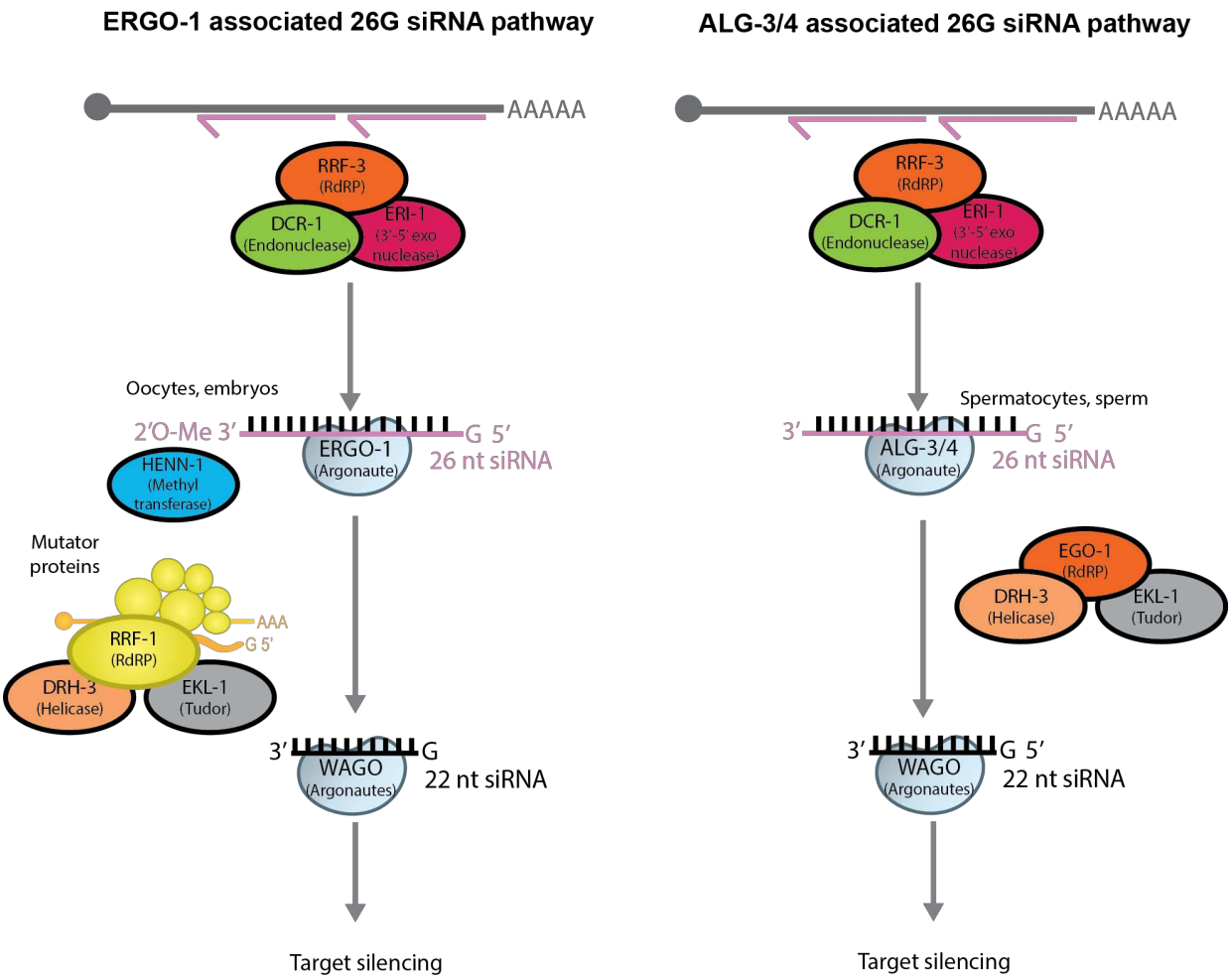

Figure 1.3. 26G RNA biogenesis in *C. elegans*. The pathway and biogenesis factors required for the formation of ERGO-1 class 26G RNAs (left) and ALG-3/4 class 26G RNAs (right). Adapted from Billi et al., 2014

gene is targeted by the RNAi pathway, it will remain silenced even after the stimulus is removed. This heritable RNAi response can be passed from parent to offspring across several generations (Buckley et al., 2012).

There is another class of noncanonical siRNAs in *C. elegans* known as CSR-1-class 22G-RNAs. Although they are similar in structure to WAGO-class 22G-RNAs, CSR-1-class siRNAs appear to function in opposition to the Mutator pathway. Rather than silencing them, CSR-1 appears to license its mRNA targets for expression by protecting them from targeting by the piRNA-dependent RNAi pathway (Claycomb et al., 2009; Seth et al., 2013; Wedeles et al., 2013).

piRNAs. PIWI-interacting RNAs (piRNAs) are, like miRNAs, transcribed by RNA polymerase II from specific loci in the genome (Billi et al., 2013; Cecere et al., 2012). Unlike miRNAs, however, piRNA maturation does not involve a double stranded foldback intermediate and is Dicer independent. The details of piRNA biogenesis vary by organism; in most animals, piRNAs are generated by a phased process called “ping-pong amplification” in which piRNAs initiate the cleavage of their target transcripts, fragments of which are matured into additional piRNAs (Ozata et al., 2019). In *C. elegans*, however, there is no known mechanism of piRNA amplification. Instead, piRNA precursors are transcribed by RNA polymerase II, trimmed down to 21 nt by nucleases, bound by the *C. elegans* PIWI homolog PRG-1, and methylated at their 3’ end (Figure 1.4) (Billi et al., 2012; Kamminga et al., 2012; Montgomery et al. 2012; Iwasaki et al., 2015). PARN-1 is the nuclease that trims the 3’ end down to its appropriate size, but the 5’ end nuclease remains unidentified (Tang et al., 2016). It is not currently known whether 3’ trimming occurs before or after loading into PRG-1.

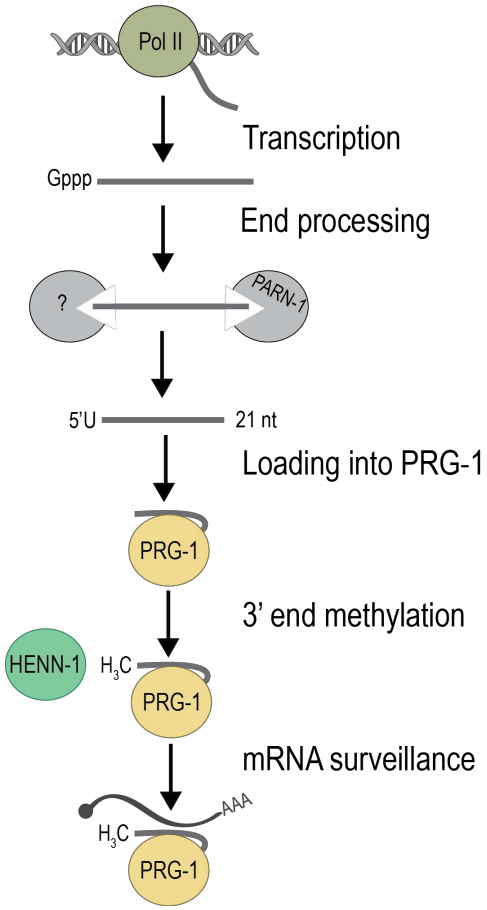

Figure 1.4. piRNA biogenesis in *C. elegans*. Model of the piRNA formation pathway from transcription to mRNA surveillance.

After maturation and loading into PIWI proteins, piRNAs perform genome surveillance, distinguishing “self” genes from “non-self” genes and protecting the genome from parasitic genetic elements such as transposons and pseudogenes (Ozata et al., 2019). For most organisms, loss of piRNAs results in immediate sterility (Thomson and Lin, 2009). Although piRNAs are important for germline immortality in worms as well, piRNA mutations in *C. elegans* result in gradual loss of fertility, with animals eventually becoming sterile after 35-80 generations (Simon et al., 2014; Heestand et al., 2018). Interestingly, piRNAs in *C. elegans* appear to target not only transposons, pseudogenes, and exogenous genetic elements such as germline transgenes, but also the majority of coding genes in the genome, and appear to be differentially expressed in the male and female germlines (Shen et al., 2018; Zhang et al., 2018; Bezler et al. 2019). Current evidence suggests that competition between the piRNA pathway and the CSR-1 22G-RNA pathway, which is thought to license mRNAs for expression, plays a role in determining which genes are expressed and which are targeted for silencing by the Mutator-dependent RNAi pathway (Shirayama et al., 2012; Seth et al., 2013).

Small RNA Methylation. In many species, certain classes of small RNAs are methylated at their 3’ end. Small RNA methylation was first identified in Arabidopsis, in which miRNAs were found to be modified by the 3'-2’-O-methyltransferase Hen1 to protect against polyuridylation and degradation (Li et al., 2005). Further investigated in flies, small RNA methylation was found to protect siRNAs and piRNAs that share perfect complementarity with their targets from degradation (Horwich et al., 2007). When a small RNA is bound to an mRNA along its entire length, the small RNA’s 3’ end is liberated from the paz domain of the Argonaute protein, as the nucleotides at the 3’

end binding to their target pulls them out of this domain and exposes the end of the small RNA. Without the protection provided by a methyl group, these exposed 3' ends are vulnerable to modification and degradation (Figure 1.1) (Horwich et al., 2007; Kawamata and Tomari, 2010). Recent work in silkworms also suggests that animals that undergo ping-pong amplification of piRNAs may differentially methylate pre-pre-piRNAs depending on the mechanism of their biogenesis, which also suggests that trimming and methylation are tightly associated (Izumi et al. 2020).

In *C. elegans*, two classes of small RNAs are known to be methylated: piRNAs and ERGO-1-class 26G-RNAs (Billi et al., 2012; Kamminga et al., 2012; Montgomery et al., 2012; Ruby et al., 2006; Vasale et al., 2010). As in other species, methylation appears to be important for stabilization of small RNAs in worms, but unlike in flies, the methylation of a small RNA does not appear to be governed by whether it is perfectly complementary to its target. piRNAs, for example, do not pair perfectly with their targets in worms, but are nonetheless methylated. There is no evidence, however, that secondary siRNAs, which do pair perfectly with their targets, are reliant on methylation (Billi et al., 2012; Kamminga et al., 2012; Montgomery et al., 2012). Additionally, the mechanism by which unmethylated primary small RNAs are destabilized in *C. elegans* remains elusive. Limited evidence suggests that, like in other organisms, polyuridylation precedes small RNA degradation in worms, but the molecular machinery responsible for the processes of both modification and degradation remains unknown (Li et al., 2005; Yu et al., 2005; Horwich et al., 2007; Saito et al., 2007; Kurth and Mochizuki, 2009; Billi et al., 2012; Kamminga et al., 2012; Montgomery et al., 2012)

RNAi in *C. elegans.* RNA interference in *C. elegans* involves numerous, spatially separated components. Situated on the cytoplasmic side of the nuclear pores of germ cells are non-membrane bound ribonucleoprotein granules called P granules (Pitt et al., 2000). P granules contain, among other components, the Argonautes PRG-1 and CSR-1, both of which contribute to RNA surveillance (Batista et al., 2008; Claycomb et al., 2009; Seth et al., 2013). mRNAs leaving the nucleus must pass through the P granule on the way to the cytoplasm to be translated and are therefore subject to surveillance. Transcripts engaged by 22G-RNAs carried by CSR-1 are licensed for translation, while those that interact with piRNAs carried by PRG-1 are marked for silencing (Shirayama et al., 2012; Seth et al., 2013; Wedeles et al., 2013). To achieve this silencing, these transcripts are shuttled into adjacent perinuclear Mutator foci, in which a complex of proteins called the Mutator complex modifies the target transcript into a substrate for its constituent RdRP, which synthesizes 22G-siRNAs antisense to the target (Aoki et al., 2007; Phillips et al., 2012; Zhang et al., 2012; Phillips et al., 2014; Tsai et al., 2015). These 22G-RNAs bind WAGO Argonautes, which then silence the target gene (Gu et al., 2009).

In addition to the piRNAs described in the example above, there are two other classes of primary small RNAs that identify targets for the RNAi pathway and initiate the production of secondary WAGO-class 22G-RNAs: exogenous siRNAs and ERGO-1 class 26G-RNAs (Billi et al., 2014; Pak and Fire, 2007; Sijen et al., 2007; Tabara et al., 2002). After the primary small RNAs initiate the silencing of a given gene, the secondary small RNAs maintain the silencing signal (Figure 1.5). Interestingly, this maintenance can be maintained even if the initiation step is disabled, allowing these secondary small

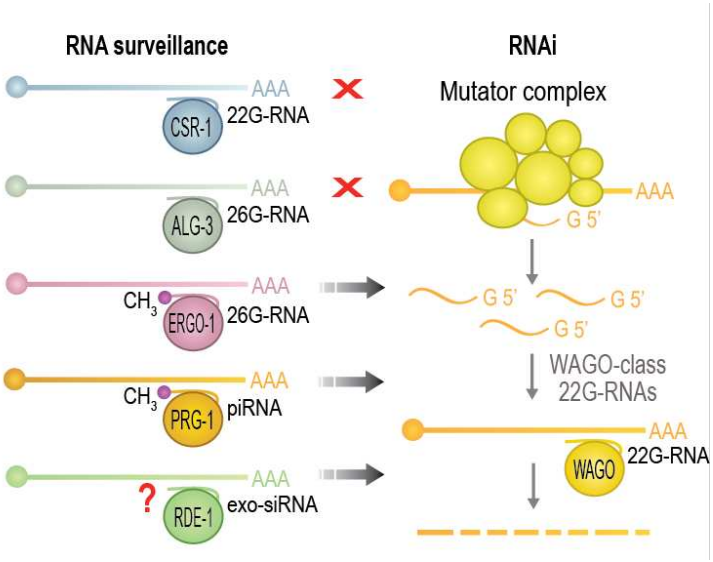

Figure 1.5. Primary small RNAs. Model depicting the interplay between RNA surveillance and WAGO-class 22G production by the RNAi pathway.

RNAs to serve not only as the effectors of gene silencing, but also as a “memory” of genes to be silenced (Shirayama et al., 2012; Buckley et al., 2012). They can even maintain a silencing signal for several generations after the stimulus that initiated it is removed through the inheritance of HRDE-1-associated 22G-siRNAs, which perform nuclear gene silencing and promote the deposition of repressive H3K9 methylation (Buckley et al., 2012).

piRNA targeting in *C. elegans*.[1] The following is an invited perspective piece written for Developmental Cell, published as written in March 2018, that details recent advances in the field of piRNA biology. It synthesizes several papers that establish rules by which mRNAs are identified for piRNA targeting.

piRNA Rules of Engagement. Germ cells are under constant attack by foreign invaders, such as transposons with the ability to self-replicate and take up residence at new locations in the genome. In animals, a major line of defense against foreign genes involves PIWI proteins and their associated Piwi-interacting RNAs (piRNAs) (Iwasaki et al., 2015). Although their role as master regulators of transposons and pseudogenes in the germline is well characterized, additional roles for piRNAs in germ cells, as well as in somatic cells, such as neurons (e.g., Kim et al., 2018), have recently come to light. *C. elegans* contains thousands of distinct piRNAs, each produced from its own autonomous transcript (Iwasaki et al., 2015). Unlike in insects and mammals, most piRNAs in *C. elegans* lack homology to transposons and rarely interact with perfect complementarity to target mRNAs (Lee et al., 2012). Thus, identifying the targets of *C.*

[1] This section was published as written:
Svendsen, J.M., and Montgomery, T.A. (2018). piRNA Rules of Engagement. Developmental Cell 44, 657-658.

elegans piRNAs has proved challenging. Now, two independent studies published in Cell (Shen et al., 2018) and Science (Zhang et al., 2018) identify targeting rules of the piRNA pathway and uncover features that help to distinguish self-genes from non-self invaders in the worm.

Many organisms, including flies, fish, and mammals, use an elaborate mechanism, termed the ping-pong cycle, to amplify the piRNA signal (Iwasaki et al., 2015). Although an analogous piRNA amplification mechanism is absent in *C. elegans*, piRNAs nonetheless propagate the silencing signal via a specialized class of small interfering RNAs (siRNAs) called 22G-RNAs. piRNA targets are handed off by the lone *C. elegans* PIWI protein, PRG-1, to a complex containing an RNA-dependent RNA polymerase that spawns out 22G-RNAs antisense to the mRNA target. Although 22G-RNAs provide a signature for piRNA targeting, there are additional triggers for 22G-RNA formation, and thus they are not always a reliable readout for piRNA activity. Furthermore, once a piRNA initiates silencing, the downstream 22G-RNAs provide a memory of targeting that can be transmitted from one generation to the next in absence of the piRNA trigger (Iwasaki et al., 2015). This phenomenon likely explains why loss of piRNAs has only a modest impact on germline development in the worm, whereas in many other animals it leads to sterility. piRNA target identification is further complicated by the 22G-RNA memory of their activity, because the impact of loss of piwi/*prg-1* on gene expression is at least partially masked by epigenetic mechanisms.

Using complementary approaches, Shen et al. (2018) and Zhang et al. (2018) set out to identify how piRNAs engage their targets in *C. elegans*. Shen et al. (2018) analyzed, transcriptome-wide, the targets of PIWI/PRG-1 using a method in which the

PRG-1-piRNA-mRNA complexes were co-immunoprecipitated and the associated RNAs ligated to one another and subjected to high-throughput sequencing (CLASH). piRNA-mRNA hybrids captured by the method allowed for identification of direct interactions between piRNAs and their mRNA targets. Surprisingly, piRNAs were found to interact with essentially all germline mRNAs. Two approaches were then used to analyze base-pairing between piRNAs and target mRNAs. The first approach involved analysis of the hybrid data to identify pairing patterns between the piRNAs and associated mRNA fragments. In the second approach, an endogenous piRNA locus was edited using CRISPR/Cas9 to produce a synthetic piRNA targeting a GFP transgene. Mutations were then introduced into the synthetic piRNA sequence to assess which positions along the piRNA were required for target recognition. A similar GFP synthetic piRNA-based approach was used by Zhang et al. (2018). Additionally, to explore endogenous targeting rules, Zhang et al. (2018) deleted an endogenous piRNA locus or, conversely, introduced a synthetic piRNA targeting endogenous genes and used the loss or gain, respectively, of 22G-RNAs as a readout for piRNA activity. Together, these experiments revealed that *C. elegans* piRNA target recognition is strikingly similar to that of miRNAs: pairing in the seed sequence (positions 2–8 relative to the 5′ end of the piRNA or miRNA) is the primary determinant of target recognition. Seed pairing, however, is not sufficient. Additional base-pairing outside of the seed is also important, particularly near the 3′ end of the piRNA (positions 14–19), which overlaps with a region important for supplementary pairing by miRNAs (positions 13–16) (Bartel, 2009) (Figure 1.6A).

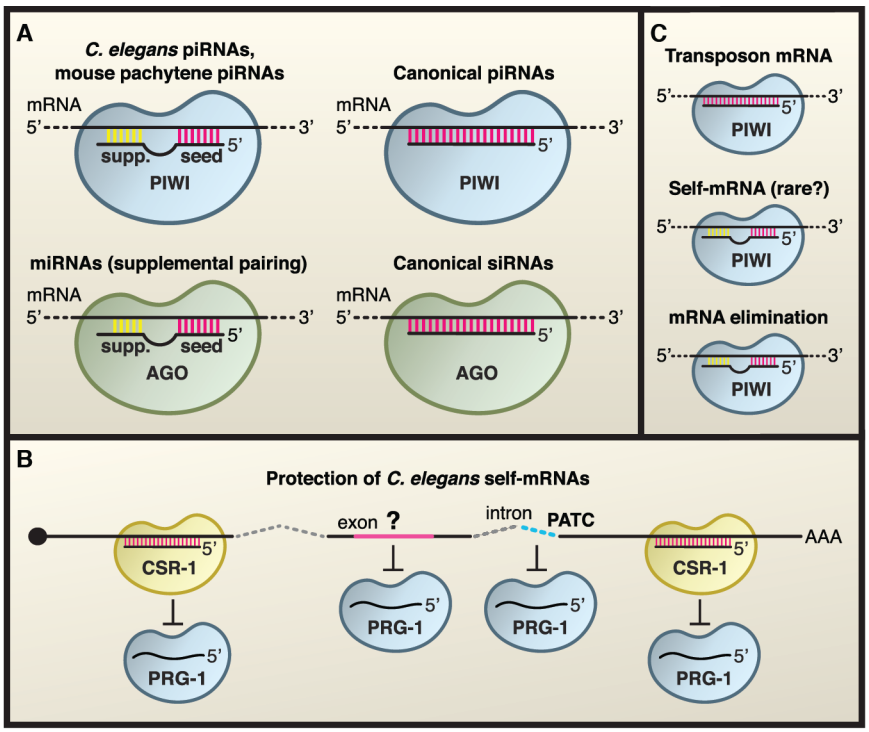

Figure 1.6. Target Recognition and Regulatory Roles of piRNAs. (A) Canonical piRNAs and siRNAs target mRNAs with perfect complementarity, whereas some piRNAs, similar to miRNAs, require only partial complementarity, particularly in the seed sequence (positions 2–8). Supplementary pairing (supp.) near the 3′ end is also important in some instances. (B) *C. elegans* safeguards against silencing of self-mRNAs via trans-acting factors (CSR-1) and cis-acting sequences (unknown exonic sequences and intronic An/Tn clusters, PATC). (C) piRNAs have essential roles in regulating transposons, typically through perfect base-pairing, and have less-understood roles in regulating self-genes and in mRNA elimination, often via imperfect pairing.

In insects and mammals, canonical piRNAs interact with perfect complementarity to their targets, similar to the way siRNAs engage their targets, often deriving from the same or related genes to those that they target (Iwasaki et al., 2015). Pachytene piRNAs in mice, however, do not appear to come from transposons and instead target a broad range of mRNAs, also using miRNA-like pairing rules, to affect widespread mRNA elimination in spermatids (Gou et al., 2014). Some Drosophila piRNAs also interact with non-transposon mRNAs through imperfect base-pairing (Iwasaki et al., 2015). Thus, the piRNA pairing rules identified in *C. elegans* may be to some extent conserved across animals.

Given the promiscuousness of *C. elegans* piRNAs, how do beneficial self-genes evade silencing? The majority of mRNAs expressed in the germline are also targeted by a distinct 22G-RNA pathway involving the worm-specific Argonaute CSR-1 (Iwasaki et al., 2015). CSR-1 targets tend to be expressed rather than silenced, pointing to a protective role of the pathway that acts in opposition to piRNAs. Indeed, by repeating their PIWI/PRG-1 CLASH experiments in a csr-1 conditional mutant background, Shen et al. (2018) showed that CSR-1 functions upstream to limit PRG-1 binding to expressed genes. It is unclear how a gene goes about obtaining protection by CSR-1. However, CSR-1 is not the only safeguard against silencing. Zhang et al. (2018) discovered that periodic adenine/thymine clusters (PATCs) found in the introns and promoters of some germline genes (Frøkjær-Jensen et al., 2016) also confer resistance to piRNAs. Another recent study (Seth et al., 2018) identified a protective role for unknown sequences within the coding regions of some endogenous genes. Thus, both

trans-acting factors, such as CSR-1, and cis-acting intrinsic sequences can safeguard against piRNAs (Figure 1.6B).

In addition to silencing non-self-genes, Shen et al. (2018) and another study from the Mello group in this issue of Developmental Cell (Tang et al., 2018) identified a role for piRNAs in fine-tuning gene expression to control sex determination in *C. elegans*. Interestingly, piRNAs also regulate sex determination in silkworms (Iwasaki et al., 2015). In both species, specific piRNAs regulate genes involved in dosage compensation. Thus, despite differences between piRNA pathways in worms and other animals, the pathways appear to share many common roles in gene regulation and genome defense (Figure 1.6C). The extent to which the promiscuous nature of *C. elegans* piRNAs is shared between other species remains to be determined.

Thesis Work. The goal of my thesis work was to better characterize the functional effects of small RNA methylation in *C. elegans*. Small RNA methylation is a widely conserved mechanism that many organisms employ to protect small RNAs from degradation, and methylation is common on animal piRNAs, the small RNAs generally responsible for maintaining germline genome integrity. Although small RNA methylation in *C. elegans* likely serves a similar purpose, little work has been done to investigate its function, especially as it relates to germline genome maintenance. Below, I summarize the gaps in the field that my thesis work is intended to fill and offer brief explanations of how filling these gaps would be valuable.

At the outset of this project, the only classes of small RNAs in *C. elegans* that were known to be methylated were piRNAs and ERGO-1 class 26G RNAs (Billi et al., 2012; Kamminga et al., 2012; Montgomery et al., 2012; Ruby et al., 2006; Vasale et al., 2010).

These RNAs have in common the fact that they interact with target mRNAs and initiate the production of secondary siRNAs antisense to them via the Mutator pathway. These are not, however, the only classes of small RNAs that act upstream of the RNAi pathway. Exogenous siRNAs, derived from dsRNA that is introduced either naturally by viral infection or uptake from the environment or experimentally by feeding RNAi treatment or injection, associate with the Argonaute RDE-1, and also initiate secondary siRNA production (Pak and Fire, 2007; Sijen et al. 2007; Tabara et al. 2002). We hypothesized that the reason primary small RNAs are methylated is related to their role in initiating RNAi. If this is true, exo-siRNAs should, like other classes of primary small RNAs, also be methylated. A comprehensive understanding of which small RNA classes require methylation would make it easier to answer the question of what methylation protects small RNAs from. If commonalities can be identified in the expression, function, and localization of these RNAs, it is possible that a common factor or function that promotes methylation can be identified. Additionally, the methylated small RNAs of *C. elegans,* piRNAs and ERGO-1-class 26G-RNAs, are expressed in the germline, and methylation may play a role in ensuring that they are able to properly regulate germline gene expression.

I was also interested in determining how small RNAs are identified for methylation. In flies, the Argonaute protein into which a small RNA is loaded determines whether it will be methylated (Ameres et al. 2010; Horwich et al. 2007). Argonaute loading comes first, followed by methylation at the 3' end. We hypothesized that Argonaute-directed methylation is conserved in worms. Additionally, if, as in flies, *C. elegans* small RNAs are methylated based on which Argonaute they are loaded into, the subpopulation of

miRNAs that associate with RDE-1 should also be methylated. Identifying a methylated subpopulation of miRNAs could have substantial implications for our understanding of miRNAs roles in *C. elegans* and contribute to a small but growing body of evidence indicating that animals employ some degree of miRNA methylation. Additionally, evidence for an Argonaute-directed model of small RNA methylation could open new avenues for studying the mechanics of small RNA methylation.

Finally, I wanted to find out why a subset of *C. elegans* small RNAs are methylated. In plants, all small RNAs (both miRNAs and siRNAs) are methylated to protect them from degradation (Li et al. 2005). In flies, piRNAs and siRNAs that are perfectly complementary to their targets need to be methylated to be protected from degradation (Horwich et al. 2007). While loss of small RNA methylation in *C. elegans* does not appear to destabilize small RNAs to the same extent that it does in other organisms, it does appear to be important for fertility. Furthermore, it is unclear what methylation protects small RNAs from. Limited evidence exists indicating a similar decay pathway to those observed in plants and flies, but the specific mechanism of degradation remains unknown (Billi et al., 2012; Kamminga et al., 2012; Montgomery et al., 2012). Additionally, while the poly(U) polymerase responsible for promoting degradation is unknown in *C. elegans* (or even whether one participates at all), the nuclease responsible for small RNA turnover has not been identified in any organism.

CHAPTER 2: *henn-1* Promotes Germline Immortality in *Caenorhabditis elegans*[1]

Summary. The germline contains an immortal cell lineage that ensures the faithful transmission of genetic and, in some instances, epigenetic information from one generation to the next. Here, we show that in Caenorhabditis elegans, the small RNA 3'-2'-O-methyltransferase *henn-1*/HEN1 is required for sustained fertility across generations. In the absence of *henn-1*, animals become progressively less fertile, becoming sterile after ~30 generations at 25°C. Sterility in *henn-1* mutants is accompanied by severe defects in germline proliferation and maintenance. The requirement for *henn-1* in transgenerational fertility is likely due to its role in methylating and, thereby, stabilizing Piwi-interacting RNAs (piRNAs). However, despite being essential for piRNA stability in embryos, *henn-1* is not required for piRNA stability in adults. Thus, we propose that methylation is important for the role of piRNAs in establishing proper gene silencing during early stages of development but is dispensable for their role in the proliferated germline.

Introduction. Piwi-interacting RNAs (piRNAs) have diverse roles in gene regulation and development but are best known for silencing transposons (Ozata et al., 2019). Loss of piRNAs often leads to sterility (Thomson and Lin, 2009). In Caenorhabditis elegans, however, disabling the piRNA pathway does not lead to immediate sterility but instead to a gradual loss of fertility over numerous generations (Heestand et al., 2018; Simon et

[1] This chapter was published as written:
Svendsen, J.M., Reed, K.J., Vijayasarathy, T., Montgomery, B.M., Tucci, R.M., Brown, K.C., Marks, T.N., Nguyen, D.A.H., Phillips, C.M., and Montgomery, T.A. (2019). *henn-1/HEN1* Promotes Germline Immortality in *Caenorhabditis elegans*. Cell Reports 29, 3187-3199.

al., 2014). *C. elegans* piRNAs initiate mRNA entry into an endogenous RNAi pathway in which small RNAs called WAGO-class 22G-RNAs are produced antisense to the mRNA target (Ashe et al., 2012; Bagijn et al., 2012; Lee et al., 2012; Luteijn et al., 2012). WAGO-class 22G-RNAs are often classified as small interfering RNAs (siRNAs), although, unlike canonical siRNAs, they are not derived from double-stranded RNA (dsRNA) and are not processed by Dicer (Ambros et al., 2003; Aoki et al., 2007; Gu et al., 2009; Pak and Fire, 2007; Sijen et al., 2007). Instead, they are produced by an RNA-dependent RNA polymerase in association with a collection of proteins called the Mutator complex (Aoki et al., 2007; Phillips et al., 2012). A subset of 22G-RNAs bind HRDE-1, a nuclear Argonaute that promotes transgenerational inheritance of RNAi and is required for transgenerational fertility (Buckley et al., 2012). The 22G-RNAs produced downstream of piRNAs, particularly those bound by HRDE-1, are thought to provide a memory of piRNA activity that seemingly persists over multiple generations, which may explain why the loss of the primary Piwi Argonaute *prg-1* does not cause immediate sterility (Ashe et al., 2012; Buckley et al., 2012; Luteijn et al., 2012; Shirayama et al., 2012).

piRNAs are methylated at their 3′ ends by the 3′-2′-O-methyltransferase HEN1 (Ozata et al., 2019). First characterized in Arabidopsis, methylation protects small RNAs from 3′–5′ trimming and decay (Billi et al., 2012; Horwich et al., 2007; Kamminga et al., 2012; Kurth and Mochizuki, 2009; Li et al., 2005; Montgomery et al., 2012; Saito et al., 2007; Yu et al., 2005). Small RNAs are bound at both their 5′ and 3′ ends by the Piwi/Argonaute they associate with. The 3′ end is anchored in the PAZ domain, which likely protects the small RNA from nucleases and other base-modifying enzymes. Small

RNAs with extensive target complementarity at their 3′ ends are released from the PAZ domain to facilitate base pairing with their targets (Kawamata and Tomari, 2010). In animals, piRNAs and siRNAs typically have extensive complementarity to their targets and are methylated, whereas miRNAs interact with only partial complementarity and are not methylated (Ozata et al., 2019). In Drosophila, methylation protects extensively base-paired small RNAs from target-directed trimming and tailing, thus explaining the link between target complementarity and methylation (Ameres et al., 2010). However, this simple complementarity rule for whether or not a class of small RNAs is methylated cannot be strictly applied to *C. elegans*, as most siRNAs, which share perfect complementarity to their targets, are not methylated (Billi et al., 2012; Kamminga et al., 2012; Montgomery et al., 2012). The only class of small RNAs, aside from piRNAs, that is thought to be methylated in *C. elegans* is one of two branches of the 26G-RNA pathway involving the Argonaute ERGO-1 (Billi et al., 2012; Kamminga et al., 2012; Montgomery et al., 2012; Ruby et al., 2006; Vasale et al., 2010).

C. elegans bearing mutations in the HEN1 ortholog *henn-1* display only modest loss of fertility under normal growth conditions (Billi et al., 2012; Kamminga et al., 2012; Montgomery et al., 2012). Here, however, we discover a critical role for *henn-1* in preserving fertility and germline integrity from one generation to the next as we explore its role in piRNA, miRNA, and RNAi pathways in the worm.

Results. *henn-1* Is Required for Transgenerational Fertility. In *C. elegans*, the Piwi ortholog *prg-1* promotes germline immortality. In the absence of *prg-1*, sterility ensues over ~35–80 generations (Simon et al., 2014). Given the presumed role of HENN-1 in methylating the 3′ ends of piRNAs to promote their stability, we used two separate

approaches to test if, like *prg-1*, *henn-1* is required for germline immortality. In the first set of experiments, modeled after Buckley et al. (2012), we measured the number of progeny produced from recently outcrossed (3×) *henn-1(pk2295)* mutants across ~28 generations at 25°C. In parallel, we measured the brood sizes of wild-type animals and freshly outcrossed (1×) *prg-1(n4357)* mutants as controls. At ~5 generations, the first generation at which measurements were taken, both *henn-1* and *prg-1* mutants displayed modest reductions in the numbers of progeny they produced relative to wild-type animals (p values = 0.00004 and 0.00002, respectively) (Figures 2.1A and S1A). By ~28 generations, the mean numbers of progeny produced by *henn-1* and *prg-1* mutants had diminished to 8 and 23, respectively, compared to 201 in wild-type (p = 0.00007 and p = 0.0002, respectively, for comparisons to wild-type), and many of the mutant animals were sterile (Figures 2.1A and S1A).

The NL4415[*henn-1(pk2295)*] strain used in these experiments has been propagated over numerous generations and may have acquired background mutations that could contribute to defects in fertility. Thus, we repeated the brood size experiments with a fresh *henn-1* deletion allele generated using CRISPR-Cas9. The new *henn-1(ram13)* allele displayed fertility rates indistinguishable from wild-type animals at ~5 generations when grown at 25°C (p = 1.0). After ~20 generations, however, animals containing the fresh *henn-1* deletion produced only 33 progeny/animal on average and

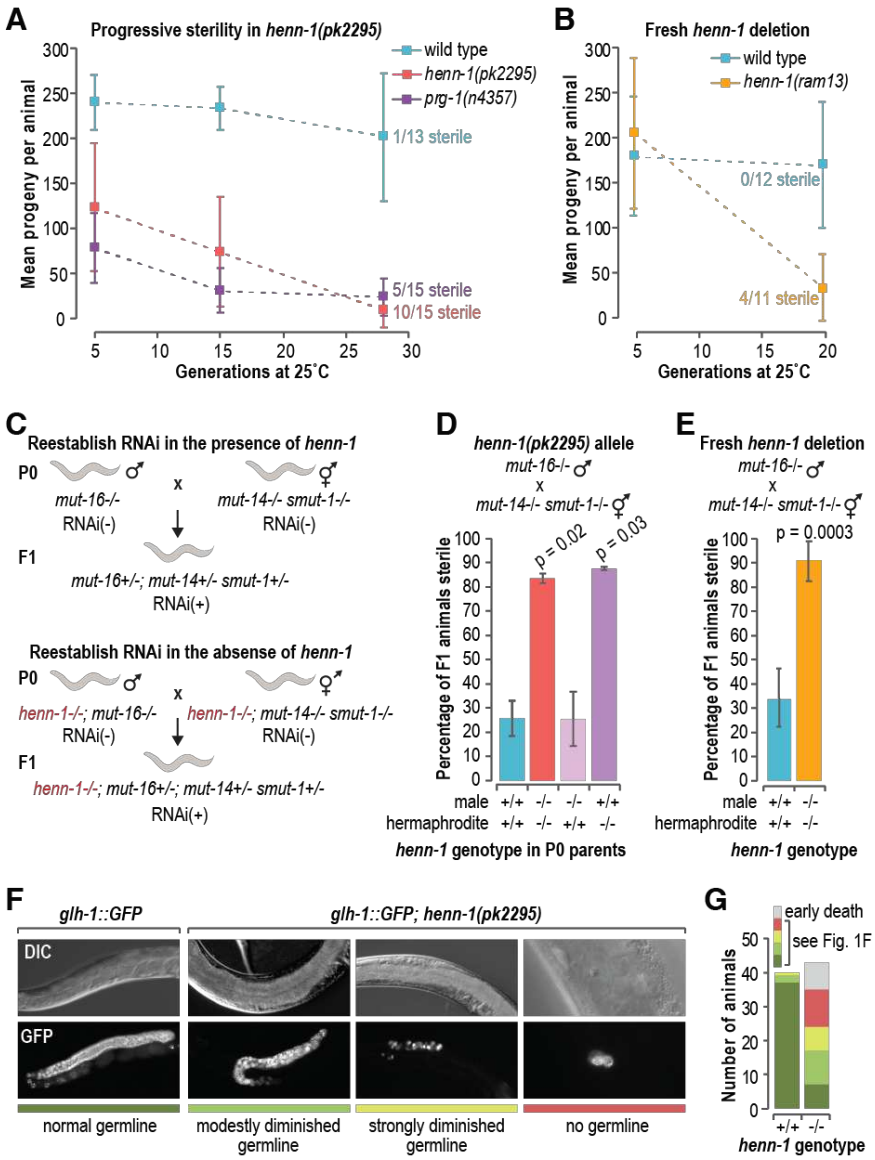

Figure 2.1. Sterility Ensues in the Absence of *henn-1*. (A) Brood sizes at ~5 generations (wild-type, n = 12; *henn-1*, n = 17; *prg-1*, n = 15), ~15 generations (wild-type, n = 10; *henn-1*, n = 15; *prg-1*, n = 13), and ~28 generations (wild-type, n = 13; *henn-1*, n = 15; *prg-1*, n = 15). The numbers of sterile animals at ~28 generations are shown. $p < 0.002$ for all comparisons to wild-type (see Figure S1A). Error bars report standard deviation. (B) Brood sizes at ~5 generations (wild-type, n = 14; *henn-1*, n = 12) and ~20 generations (wild-type, n = 12; *henn-1*, n = 11). The numbers of sterile animals at ~20 generations are shown. Individual data points and p values are in Figure S1B. Error bars report standard deviation. (C) The genetics-based approach used to reestablish WAGO-class 22G-RNA production and, thus, endogenous RNAi in *henn-1*$^{+/+}$ or *henn-1*$^{-/-}$ animals. RNAi competency is indicated by RNAi+ or RNAi−. (D) Mean percentage of F1 progeny from the crosses illustrated in (C) that were sterile (n = 2 biological replicates each assaying the progeny from 7–27 crosses). Error bars

report standard deviation. (E) Same as in (D) but with the *henn-1(ram13)* allele. The *henn-1* genotype is indicated and because both parents are homozygous mutant or wild-type for *henn-1*, the genotype applies to both the P0 parents and the F1 progeny (n = 4 independent experiments each assaying the progeny from 11–34 crosses). Error bars report standard deviation. (F) Differential interference contrast (DIC) and GFP fluorescence images of the diminutive germlines of sterile *glh-1::GFP; henn-1(pk2295)* animals. An image of the germline of a *glh-1::GFP* animal wild-type for *henn-1* is shown as a control. Strains were grown at 25°C for 10 generations. The colored bars under the images relate to the key in (G). (G) Numbers of *henn-1*$^{+/+}$ and *henn-1*$^{-/-}$ animals displaying germline defects exemplified in (F), as indicated in the key.

exhibited a high incidence of sterility, whereas wild-type animals produced 169 progeny on average and were all fertile ($p = 0.0009$ for comparison to wild-type) (Figures 2.1B and S1B).

We then used a second assay for transgenerational fertility, modeled after Simon et al. (2014), in which we followed the fertility of 10 independent *henn-1(pk2295)* and *prg-1(n4357)* mutant lines, scoring at every generation whether or not each line was fertile. All of the *henn-1* mutant lines had become sterile by 29 generations at 25°C (Figure S1C). However, sterility occurred after only 12 generations in *prg-1* mutants (Figure S1C). Additionally, *prg-1* mutants displayed progressive sterility at 20°C across 30 generations, whereas *henn-1* mutants did not (Figure S1D).

To determine if the 3′-2′-O-methyltransferase activity of *henn-1* is required for transgenerational fertility, we tested whether animals containing a mutation that disrupts the catalytic site of *henn-1* also display a progressive decline in fertility. Indeed, between 1 and 10 generations at 25°C, *henn-1(pk2452)* mutants displayed an ~55% reduction in the mean number of progeny they produced ($p = 0.0072$) (Figure S1E). Finally, to determine if defects in piRNA function are likely responsible for the transgenerational sterility of *henn-1* mutants, we assessed whether the loss of the other class of small RNAs presumed to be methylated in *C. elegans*, ERGO-1-class 26G-RNAs, affects fertility. Mutations in *ergo-1* did not cause transgenerational sterility (Figures S1C and S1D). Therefore, our results suggest that *henn-1*, and hence presumably methylation, is important for the role of piRNAs in maintaining germline immortality, although it is possible that *henn-1* has additional unknown roles that contribute to its phenotype.

Sterility Ensues after Reestablishing WAGO-Class 22G-RNA Production in the Absence of *henn-1.* Disabling both the piRNA pathway and the WAGO-class 22G-RNA pathway and then restoring just the WAGO pathway causes sterility, despite neither pathway being essential for fertility under normal conditions (de Albuquerque et al., 2015; Phillips et al., 2015). In the animals in which the WAGO pathway is restored in the absence of piRNAs, essential genes are misrouted into the RNAi pathway for silencing (de Albuquerque et al., 2015; Phillips et al., 2015). It is not clear if this role for piRNAs in preventing silencing of essential genes is related to its role in maintaining germline immortality. However, given that *henn-1* is required for piRNA stability, we tested if it is also required for fertility upon reestablishing the WAGO pathway. To reestablish the WAGO pathway, we crossed two strains containing distinct mutations, *mut-16* or *mut-14 smut-1*, that cause loss of WAGO-class 22G-RNAs, such that their progeny received functional copies of *mut-14* and *smut-1* from one parent and a functional copy of mut-16 from the other parent. Thus, although neither parent was capable of WAGO-class 22G-RNA formation, the pathway was restored in their progeny (Figure 2.1C). If *henn-1* is required for the role of piRNAs in establishing proper RNA silencing, we would predict that introducing a *henn-1* mutation into the two strains used to reestablish the WAGO pathway would lead to sterility in the offspring of the cross, as we previously showed occurs when the two strains contain mutations in *prg-1* (Phillips et al., 2015). Indeed, the vast majority of *henn-1* mutants in which WAGO-class 22G-RNA production was restored were sterile, whereas, in the presence of *henn-1*, most animals were fertile ($p = 0.02$ for the differences between *henn-1*+/+ and *henn-1*−/−) (Figure 2.1D).

Reactivating WAGO-class 22G-RNA production causes sterility specifically in the absence of maternally contributed *prg-1* (de Albuquerque et al., 2015; Phillips et al., 2015). To determine if, similarly, a maternal contribution of *henn-1* is specifically required for fertility when reestablishing WAGO-class 22G-RNA production, we set up crosses to reactivate the WAGO pathway in which only one parent was mutant for *henn-1*. The progeny of animals that received a paternal, but not a maternal, contribution of wild-type *henn-1* were mostly sterile (Figure 2.1D). In contrast, progeny that received a maternal contribution of wild-type *henn-1*, regardless of whether they received a paternal contribution of wild-type *henn-1*, were mostly fertile, indicating that, like *prg-1*, a maternal contribution of *henn-1* is required for fertility when reestablishing WAGO-class 22G-RNA production (Figure 2.1D). It is unlikely that background mutations are responsible for the sterility that ensues after restoring the WAGO pathway, as both old and new alleles of *henn-1* displayed similar proportions of sterile animals (~83%–90%) (Figures 2.1D and 2.1E).

We next assessed whether *henn-1* mutants display germline atrophy or defects in germ cell proliferation similar to those exhibited by *prg-1*/piwi mutants as they go sterile either over multiple generations or upon reestablishing WAGO-class 22G-RNA production (de Albuquerque et al., 2015; Heestand et al., 2018; Phillips et al., 2015). To do so, we introduced a germ cell marker, glh-1::GFP (Andralojc et al., 2017), into *henn-1(pk2295)* mutants and examined adult animals after several generations at 25°C. At ten generations, many of the glh-1::GFP; *henn-1(pk2295)* mutants were sterile and displayed diminutive and underproliferated germlines reminiscent of sterile *prg-1* mutants (Figures 2.1F and 2.1G) (de Albuquerque et al., 2015; Heestand et al., 2018;

Phillips et al., 2015). Thus, *henn-1* is required for proper maintenance of the germline over multiple generations. That *henn-1* and *prg-1* have a similar impact on germline integrity is further evidence that *henn-1* is important for the role of piRNAs in preserving generational fertility.

***henn-1* Impacts WAGO-Class 22G-RNA Formation throughout Development.** *henn-1* is required for piRNA accumulation in embryos and L1 larvae but mostly dispensable later in development (Billi et al., 2012). This suggests that methylation may not be required for piRNA stability in the proliferating germline. To assess the impact of *henn-1* on piRNA stability in the germline, we sequenced small RNAs from dissected distal gonads of adult animals, which are comprised primarily of germ cells (Pazdernik and Schedl, 2013), from wild-type and *henn-1* mutants. We also sequenced small RNAs from mixed-stage embryos, which have a variable number of somatic cells but contain only two germline precursor cells. To determine if piRNAs are more susceptible to decay in the germline precursor cells of embryos compared to the proliferated germlines of adults, an indicator of which is trimming or truncation at the 3′ ends, we calculated the proportions of piRNA reads that displayed 1- to 5-nt truncations in our high-throughput sequencing libraries. In *henn-1* mutant embryos, we observed an ~2.9-fold increase in the proportion of piRNAs that were truncated relative to wild type ($p = 0.00005$), whereas in gonads, we observed a more modest 1.5-fold increase ($p = 0.002$) (Figures 2.2A and 2.2B). piRNA trimming in gonads was almost exclusively limited to 1 nt, whereas in embryos we observed 1- to 2-nt truncations (Figure 2A). To determine if the elevated levels of piRNA truncations in *henn-1* mutants corresponded to a reduction in mature piRNA levels, we used TaqMan qRT-PCR, to measure the levels of three

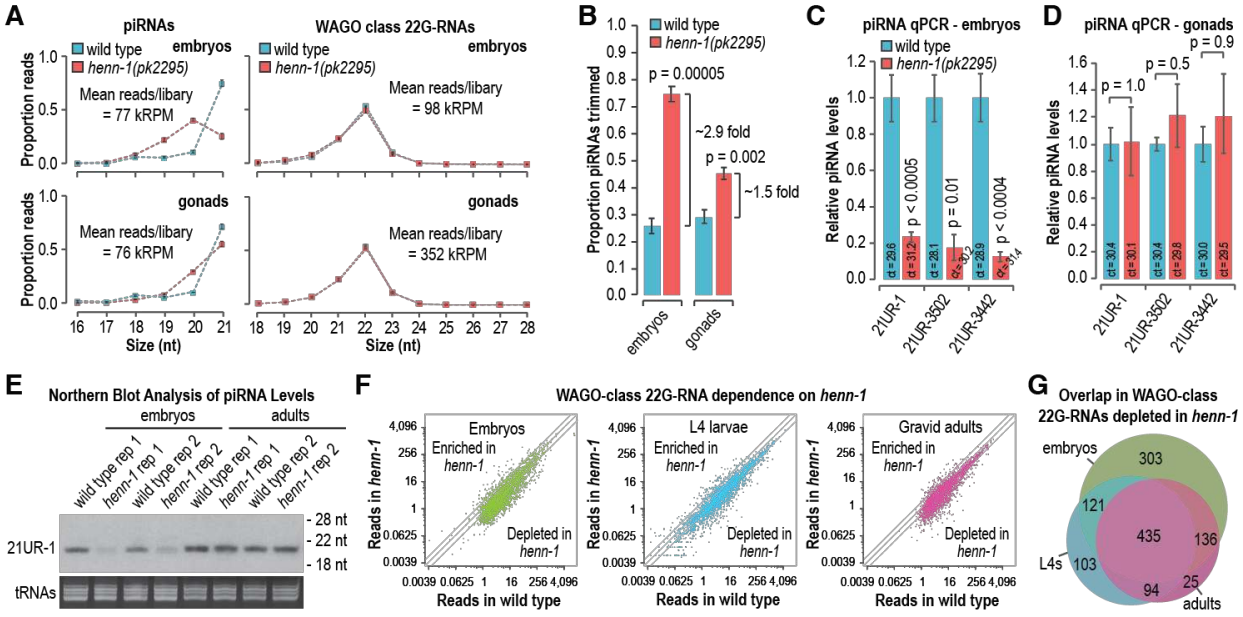

Figure 2.2. Requirement for *henn-1* in piRNA Stability and WAGO-Class 22G-RNA Production. (A) The proportions of total high-throughput sequencing reads for piRNAs and WAGO-class 22G-RNAs in embryos and dissected gonads are plotted by size. Mean reads per library are shown as thousand reads per million total mapped reads (kRPM) (n = 3 biological replicates). Error bars report standard deviation. (B) The proportions of total piRNA reads that display 1- to 5-nt truncations (mean trimmed reads/total reads) in embryos and dissected gonads (n = 3 biological replicates). Error bars report standard deviation. (C and D) qRT-PCR assay of three piRNAs in embryos (C) and dissected gonads (D) (n = 3 biological replicates for each assay). The mean cycle threshold (ct) value is shown for each assay. piRNA ct values were normalized to miR-35 ct values. Error bars report standard deviation. (E) Northern blot of the piRNA 21UR-1 in embryos and adults. Ethidium bromide (EtBr)-stained tRNAs are shown as a loading control. Two of three biological replicates are shown. (F) Normalized WAGO-class 22G-RNA reads (reads per million total mapped reads) in wild type (x axis) and *henn-1(pk2295)* (y axis). Data from embryos, L4 larvae, and gravid adults are shown (no biological replicates). (G) Venn diagram displaying the overlap in genes depleted of WAGO-class 22G-RNAs by >50% in *henn-1(pk2295)* embryos, L4 larvae, and adults.

piRNAs. Unlike high-throughput sequencing library preparation, TaqMan small RNA qRT-PCR is not thought to be hindered by 3′ methylation. Each of the piRNAs tested was strongly depleted in *henn-1* mutant embryos, indicating that the relatively high levels of truncations we observed in embryos were coincident with their decay ($p \leq 0.01$) (Figure 2.2C). In contrast, we did not detect any differences in piRNA levels in *henn-1* mutant gonads, despite the modest increase we observed in piRNA trimming ($p = 0.5–1.0$) (Figure 2.2D). To confirm our qRT-PCR results, we examined 21UR-1 by northern blot. Consistent with our qRT-PCR results, 21UR-1 levels were strongly depleted in *henn-1*-mutant embryos but appeared unchanged in *henn-1*-mutant adults relative to wild-type animals (Figure 2.2E). Our results suggest that *henn-1*, and thus presumably methylation, is important for protecting piRNAs from decay in early embryos but is largely dispensable in the proliferated germline of adult animals.

piRNAs trigger secondary siRNA (WAGO-class 22G-RNA) production from their targets, and consequently, 22G-RNA production from many WAGO target genes is reduced in *prg-1* mutants (Lee et al., 2012). To identify the requirement for *henn-1* in triggering WAGO-class 22G-RNA production, we subjected small RNAs from wild-type and *henn-1(pk2295)* mutant embryos, L4 larvae, and gravid adults to high-throughput sequencing. In each of the developmental stages, we observed a similar modest loss of 22G-RNAs from WAGO targets in *henn-1* mutants (Figure 2.2F). Consistent with previous studies, WAGO-class 22G-RNAs did not display 3′ truncations in the absence of *henn-1*, indicating that they are indirectly affected by loss of *henn-1* activity (Figure 2.2A) (Billi et al., 2012; Kamminga et al., 2012; Montgomery et al., 2012). A total of ~75% of WAGO targets depleted of 22G-RNAs in *henn-1* mutant adults were also

depleted of 22G-RNAs in *prg-1* mutants, indicating that *henn-1* primarily affects piRNA-dependent 22G-RNAs (Figure S2) (Phillips et al., 2015). The majority of WAGO target genes depleted of 22G-RNAs >50% in embryos were also depleted of 22G-RNAs >50% in adults and L4 stage larvae (Figure 2.2G). These results suggest that *henn-1* impacts piRNA-dependent 22G-RNA production throughout development despite the requirement for *henn-1* in piRNA stability being restricted to early stages of development.

Loss of *henn-1* has little impact on gene expression in the germline

because the loss of *henn-1* has a modest impact on the health of animals grown at 20°C (Billi et al., 2012; Kamminga et al., 2012; Montgomery et al., 2012), we could examine its role in regulating gene expression in the germline, where piRNAs are active, without developmental defects confounding the results. However, a caveat to this approach is that *henn-1* is not required for piRNA stability in adults, the stage at which we are able to dissect germline tissue. Nonetheless, because many piRNA-dependent 22G-RNAs are depleted in *henn-1* mutant adults at 20°C, we could then assess the impact of their loss on germline gene expression. Therefore, we did mRNA sequencing using the same wild-type and *henn-1(pk2295)* RNA samples from adult gonads that were used for the small RNA high-throughput sequencing analysis described above (Figures 2.2A and 2.2B). We then performed differential gene expression analysis applying an arbitrary 1.3-fold change cutoff, which excludes many genes that are differentially expressed based on a false discovery rate of 0.05 but which increases the likelihood that differences observed are biologically relevant. As we predicted based on the health of the animals at 20°C, only modest changes in mRNA

expression were observed in *henn-1* mutants relative to wild-type animals, with 238 genes significantly upregulated and 50 genes significantly downregulated >1.3-fold (Figure 2.3A; Table S1).

In parallel, we performed differential expression analysis of small RNAs from these samples, which we had earlier used in our trimming analysis, to assess more comprehensively the impact of *henn-1* on 22G-RNA levels. We identified 1,084 WAGO target genes that were depleted of 22G-RNAs >1.3-fold (Figure 2.3B; Table S2). A small subset of genes targeted by CSR-1, an Argonaute implicated in licensing genes for expression (Claycomb et al., 2009; Seth et al., 2013; Wedeles et al., 2013), also displayed altered levels of 22G-RNAs (Figure 2.3B; Table S2). piRNA levels in our sequencing data appeared elevated in *henn-1* mutants, likely due to increased capture efficiency, as 3′-2′-O-methylation inhibits RNA ligation and reverse transcription during library preparation, despite our efforts to minimize such biases (Table S2) (Munafó and Robb, 2010).

Among the upregulated genes, 20% are histones, representing each of the core families—H2A, H2B, H3, and H4 (Figures 2.3C and S3A; Table S1). As these are multicopy gene families and the effects are modest (1.35- to 1.86-fold), it is unclear what impact this might have on the chromatin landscape. A small subset of histone genes had reduced levels of 22G-RNAs in *henn-1* mutants, suggesting that *henn-1*-dependent 22G-RNAs may have a role in regulating histones, although it is possible that altered cell physiology in *henn-1* mutants indirectly impacts histone levels (Figure S3A; Table S2). The levels of several genes involved in RNAi—*sid-1*, *rde-11*, and *wago-4*—were modestly reduced in *henn-1* mutants, each of which also had reduced levels in

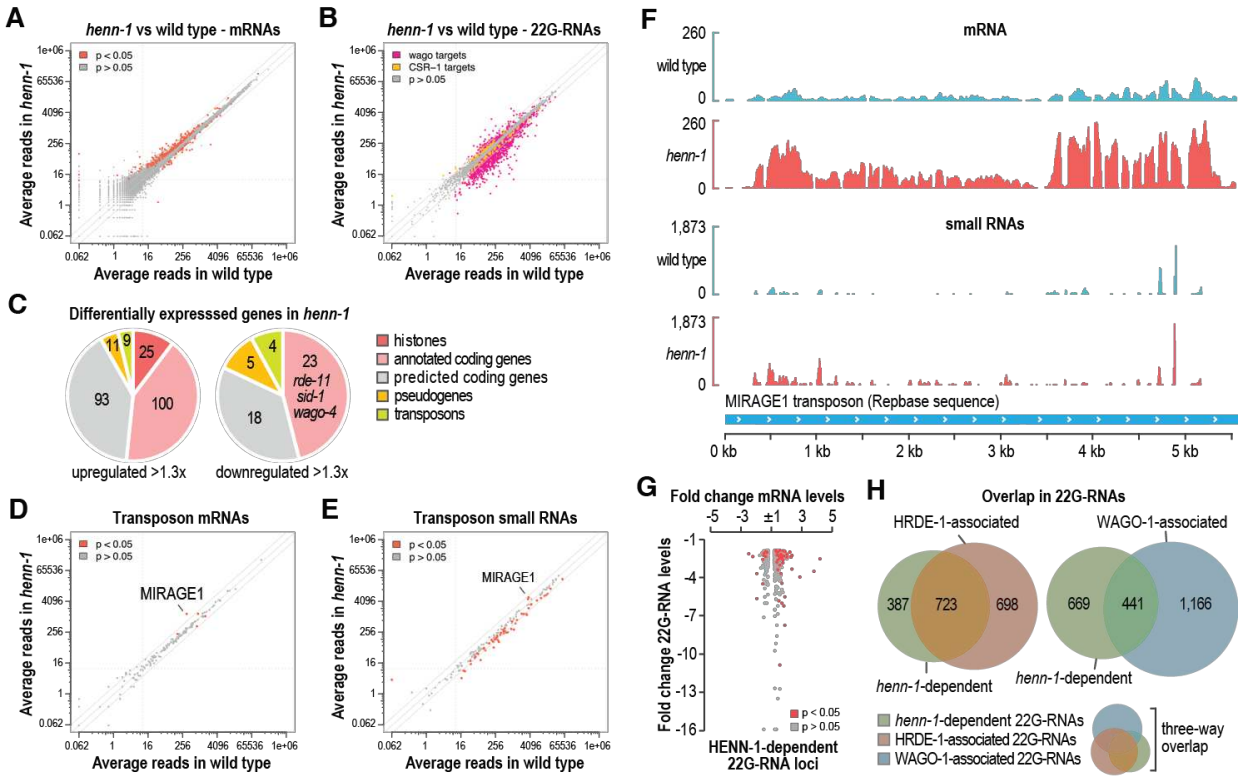

Figure 2.3. Differential Expression of mRNAs and Small RNAs in *henn-1* Gonads. (A) Scatterplot displaying each gene as the average number of normalized reads in wild type (x axis) and *henn-1(pk2295)* (y axis) (n = 3 biological replicates). Grey lines are at −2-, 1-, and 2-fold change relative to wild type. Dashed lines are at 10 reads on each axis. (B) Scatterplot displaying each WAGO and CSR-1 target gene as the average number of normalized small RNA reads in wild type (x axis) and *henn-1(pk2295)* (y axis) (n = 3 biological replicates). (C) Pie charts displaying the proportions of genes upregulated or downregulated in *henn-1(pk2295)* ($p < 0.05$) belonging to each of the indicated classes. (D) Scatterplot displaying each transposon family as the average number of normalized mRNA reads in wild type (x axis) and *henn-1(pk2295)* (y axis) (n = 3 biological replicates). (E) Scatterplot displaying each transposon family as the average number of normalized small RNA reads in wild type (x axis) and *henn-1(pk2295)* (y axis) (n = 3 biological replicates). (F) mRNA and small RNA read distribution across the MIRAGE transposon consensus sequence. One of three biological replicates is shown. (G) Scatterplot displaying fold change in mRNA levels in *henn-1(pk2295)* relative to wild type for each gene depleted of 22G-RNAs >1.3-fold in *henn-1(pk2295)*. (H) Venn diagrams displaying the overlap between genes depleted of 22G-RNAs in *henn-1(pk2295)* and genes that yield 22G-RNAs enriched >1.3-fold in WAGO-1 or HRDE-1 coIPs. The three-way Venn diagram is a combination of the two-way Venn diagrams.

henn-1 in a microarray-based study using whole animals (Figures 2.3C and S3B-S3D; Table S1) (Kamminga et al., 2012). *sid-1* and *rde-11* are required for optimal exogenous RNAi, and their downregulation could explain the reduced RNAi efficiency previously observed in *henn-1* mutants (Billi et al., 2012; Kamminga et al., 2012; Winston et al., 2002; Yang et al., 2012; Zhang et al., 2012). WAGO-4 transports siRNAs from parent to progeny to promote multigenerational RNAi, and thus, its misregulation may have a role in the transgenerational sterility of *henn-1* mutants (Wan et al., 2018; Xu et al., 2018). However, wago-4 levels were reduced by only ~1.3-fold in *henn-1* mutants, suggesting that other factors likely contribute to the transgenerational sterility of *henn-1* mutants.

As piRNAs are well known for their role in regulating transposons, we used a more targeted approach to assess the role of *henn-1* in transposon regulation. We aligned our RNA sequencing (RNA-seq) reads from wild-type and *henn-1* mutants to each of 152 transposon family consensus sequences and compared the levels of small RNAs and mRNAs produced from each family (Jurka, 2000). Only five transposon families were misregulated in *henn-1* mutants, most notably MIRAGE, which was upregulated ~4-fold and is also upregulated in *prg-1* mutants (Figure 2.3D; Table S3) (McMurchy et al., 2017). Desilencing of MIRAGE is partially responsible for the sterility of several heterochromatin factor mutants linked to small-RNA-mediated gene silencing (McMurchy et al., 2017). Most 22G-RNAs produced from MIRAGE were upregulated in *henn-1*, contrary to what would be expected if these siRNAs were involved in RNA silencing (Figures 2.3E and 2.3F; Table S3). It is possible that MIRAGE is indirectly affected by *henn-1*, although given that it is also upregulated in *prg-1* mutants, it may be that other elements of the pathway obscure the relationship between 22G-RNA

production and RNA silencing. We, therefore, examined the relationship between *henn-1*-dependent 22G-RNAs and mRNA misregulation in *henn-1* mutants more generally. Genes depleted of 22G-RNAs in *henn-1* mutants had a tendency to be upregulated, although there was considerable variation and some were instead downregulated (Figure 3G). This inconsistency could be due to complex feedback between mRNA expression and 22G-RNA production. The numbers of predicted piRNA target sites in mRNAs misregulated in *henn-1* mutants, as determined by sequence complementarity and by PRG-1-mRNA co-immunoprecipitation (coIP) (CLASH), were similar between genes that were upregulated and those that were downregulated (Table S1) (Shen et al., 2018; Wu et al., 2019; Zhang et al., 2018). However, all but one misregulated gene had multiple predicted piRNA target sites in at least one of the two target prediction methods, and it is not clear which genes are bona fide piRNA targets (Table S1). Further studies exploring the relationship between piRNA-mRNA interactions and gene expression may shed light on these results.

HRDE-1 is a nuclear Argonaute that associates with a subset of WAGO-class 22G-RNAs and is required for RNAi inheritance, piRNA-mediated transgenerational gene silencing, and at 25°C for transgenerational fertility (Ashe et al., 2012; Buckley et al., 2012; Luteijn et al., 2012; Shirayama et al., 2012). Because *henn-1* is also required for transgenerational fertility at 25°C and for piRNA stability and may, therefore, promote the production of HRDE-1-associated 22G-RNAs, we examined the overlap between 22G-RNAs that are *henn-1*-dependent and those that associate with HRDE-1 or with WAGO-1, a WAGO Argonaute not implicated in transgenerational inheritance. Of the ~1,100 genes depleted of 22G-RNAs in *henn-1* mutants, ~66% were enriched for 22G-

RNAs that co-immunoprecipitated (coIP'd) with a FLAG::HRDE-1 fusion protein (Figure 3H; Table S4). Only ~40% were enriched for 22G-RNAs that coIP'd with GFP::FLAG::WAGO-1, the majority of which also coIP'd with HRDE-1 (Figure 2.3H; Table S4).

Together, our results indicate that *henn-1* is important for the production of piRNA-dependent and HRDE-1-associated 22G-RNAs. However, the consequence of the loss of *henn-1* on gene expression in the adult germline is modest under the optimal growing conditions in which our experiments were done. Given that growth at elevated temperatures over multiple generations exacerbates the *henn-1* phenotype, more dramatic defects in gene expression almost certainly underlie the progressive sterility of *henn-1* mutants. Unfortunately, the severe germline defects that occur under such conditions would complicate germline dissections and confound RNA-seq analysis of gene expression.

Exogenous siRNAs Are Modified at Their 3′ Ends. Both classes of small RNAs that are presumably methylated in *C. elegans*, piRNAs, and ERGO-1-class 26G-RNAs are thought to function primarily to trigger WAGO-class 22G-RNA production (Figure 2.4A) (Billi et al., 2014). Thus, we hypothesized that methylation is specific to small RNAs that act upstream of the WAGO pathway. Exogenous siRNAs produced from dsRNA administered during RNAi treatment bind to the Argonaute RDE-1 and like piRNAs and ERGO-1-class 26G-RNAs act as primary small RNAs to trigger 22G-RNA production (Pak and Fire, 2007; Sijen et al., 2007; Tabara et al., 2002). If methylation is specific to primary small RNAs upstream of WAGO-class 22G-RNAs, exogenous siRNAs should also be methylated. To address this, we did RNAi against the endogenous gene pos-1

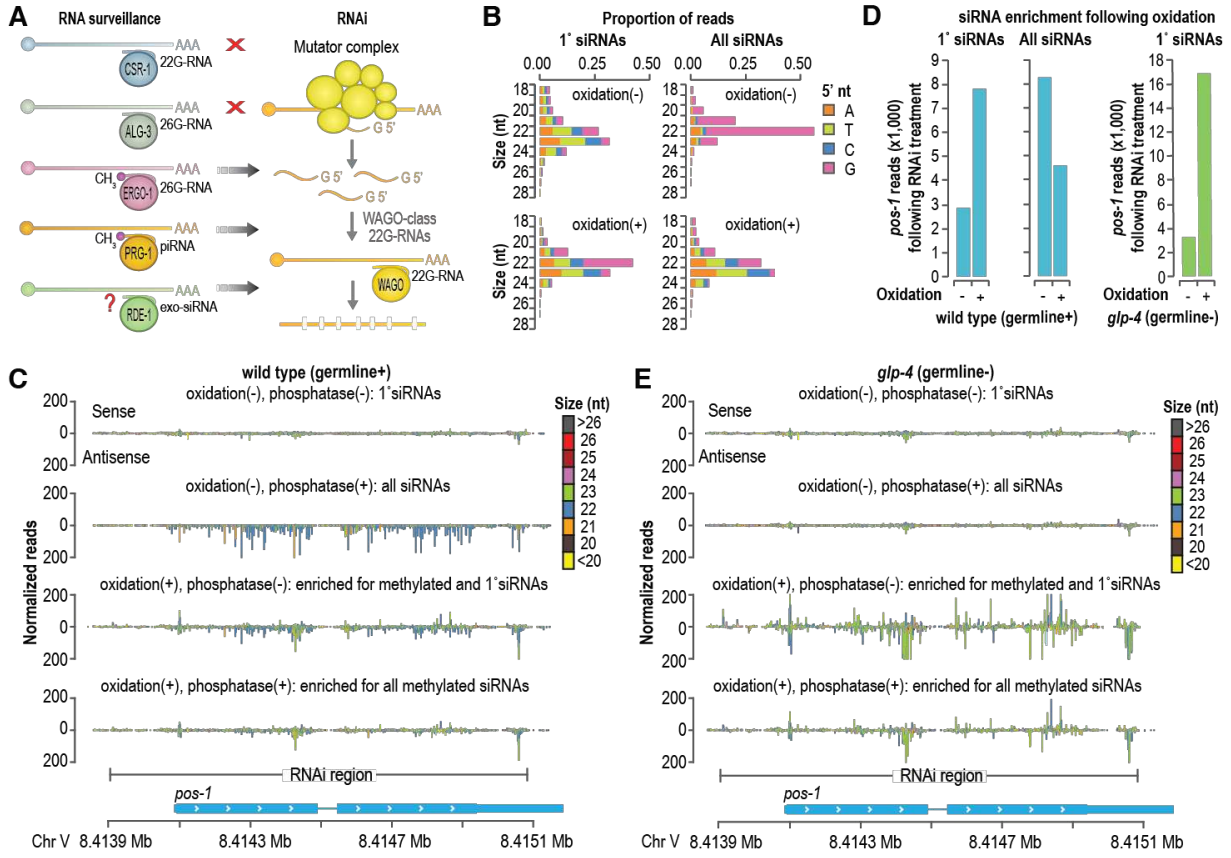

Figure 2.4. Primary siRNAs Are Modified at Their 3′ Ends. (A) Model depicting the interplay between RNA surveillance and WAGO-class 22G-RNA production by the RNAi pathway. (B) Size distribution and 5′ nucleotide composition of *pos-1* siRNAs following *pos-1* RNAi, as determined by high-throughput sequencing. Small RNAs were treated with sodium periodate (oxidation) to enrich for methylated small RNAs or subjected to a control treatment prior to library preparation. The “1° siRNAs” plot corresponds to libraries in which the small RNAs were not treated with RNA 5′ polyphosphatase and, thus, do not include di- and tri-phosphorylated small RNAs (e.g., 22G-RNAs). The “All siRNAs” plot corresponds to libraries in which the small RNAs were treated with RNA 5′ polyphosphatase and, thus, include both 1° and 2° siRNAs. (C) Small RNA read distribution across *pos-1* from wild-type high-throughput sequencing libraries in which the small RNAs were treated with sodium periodate (oxidation +) and RNA 5′ polyphosphatase (polyphosphatase +) as indicated. (D) Bar plots displaying normalized reads (reads per million total mapped reads) mapping to *pos-1* following sodium periodate (oxidation +) or control treatment (oxidation −). The plots on the left are from wild-type animals, and the plot on the right is from *glp-4(bn2)* mutants, which lack proliferated germlines and for which only primary siRNAs are shown. (E) Small RNA read distribution across *pos-1* from *glp-4(bn2)* high-throughput sequencing libraries in which the small RNAs were treated with sodium periodate (oxidation +) and RNA polyphosphatase (polyphosphatase +) as indicated.

in wild-type animals and tested whether primary and secondary siRNAs (i.e., WAGO-class 22G-RNAs) corresponding to pos-1 were modified at their 3′ ends by using a high-throughput sequencing approach. To enrich for small RNAs containing 3′ modifications, a fraction of the small RNA sample from animals undergoing pos-1 RNAi was treated with sodium periodate, an oxidizing agent that disrupts the 3′ base of unmethylated, but not 2′-O-methylated, small RNAs, thereby inhibiting adaptor ligation to the 3′ end (Seitz et al., 2008). Although sodium periodate treatment does not directly assess methylation, it is a widely used proxy that is not known to be confounded by other small RNA chemical modifications (Yu and Chen, 2010). The other fraction was treated similarly but was not oxidized. Each of the two fractions was further split between an RNA 5′ polyphosphatase treatment, which reduces the triphosphate group found on 22G-RNAs to monophosphate, thereby enabling capture by 5′ ligation during small RNA library preparation (Pak and Fire, 2007; Sijen et al., 2007), and a control treatment. The fractions treated with RNA 5′ polyphosphatase would presumably yield mostly 22G-RNAs, as this class of small RNAs is far more abundant than primary siRNAs (Pak and Fire, 2007; Sijen et al., 2007). The fractions that were not treated with RNA 5′ polyphosphatase would likely exclude 22G-RNAs because of an adaptor-ligation-incompatible 5′ triphosphate group. The four small RNA fractions were subjected to library preparation and high-throughput sequencing.

Small RNAs derived from pos-1 in both oxidized and non-oxidized libraries in which the small RNAs were not treated with RNA 5′ polyphosphatase displayed features associated with primary siRNAs: similar proportions of 22- and 23-nt species, little or no bias for a 5′ G, and production from both sense and antisense strands of the dsRNA

administered to the animals to elicit RNAi (Figures 2.4B and 2.4C) (Zhang et al., 2012). These presumptive primary siRNAs were enriched >2-fold by oxidation, indicating that at least a subset is modified at their 3′ ends (Figure 2.4D). Libraries in which the small RNAs were not subjected to oxidation but were treated with RNA 5′ polyphosphatase displayed strong enrichment of small RNAs with features characteristic of 22G-RNAs: predominant length of 22 nts, strong bias for a 5′G, and production antisense to pos-1 mRNA (Figures 2.4B and 2.4C). Oxidation of small RNAs treated with RNA 5′ polyphosphatase caused a depletion in these presumptive secondary siRNAs derived from pos-1 (Figure 2.4D). Furthermore, the length, 5′ nt distribution, and strand polarity of the small RNAs in this library resembled that of primary siRNAs, indicating that the more abundant 22G-RNAs were depleted and, hence, largely unmethylated (Figures 2.4B and 2.4C). In parallel, we assessed whether primary siRNAs are specifically modified in the germline or if somatic siRNAs are also modified. In *glp-4(bn2)* animals, which fail to undergo germline proliferation when grown at 25°C (Beanan and Strome, 1992), we did not capture small RNAs aligning to pos-1 that resembled 22G-RNAs (i.e., 22-nt-long reads containing a 5′G) regardless of whether the small RNAs were treated with RNA 5′ polyphosphatase (Figure 2.4E). This is likely because pos-1 is expressed in the germline and, as a consequence, germline-less *glp-4* mutants lack an mRNA template for 22G-RNA production. Primary siRNAs, which are derived from the dsRNA administered to the animals and, therefore, not dependent on an endogenous mRNA template, were strongly enriched by oxidation, suggesting that at least a subset of somatic primary siRNAs is also modified (Figures 2.4D).

We next assessed whether the 3′ modification that we identified on primary siRNAs is dependent on *henn-1* by sequencing small RNAs from wild-type and *henn-1(pk2295)* mutant animals undergoing pos-1 RNAi. As before, the small RNAs were split into oxidized and non-oxidized fractions; however, each fraction was treated with RNA 5′ polyphosphatase and, thus, both primary and secondary siRNAs were captured. Nonetheless, we could distinguish primary siRNAs from secondary siRNAs by their polarity, as any sense-strand siRNAs are presumably produced from the dsRNA administered to the animals and are, thus, primary siRNAs. In wild-type animals, sense strand siRNAs were enriched ~5-fold in the library from oxidized small RNAs relative to the non-oxidized counterpart, consistent with our earlier conclusion that primary siRNAs are modified (Figure S4). In *henn-1(pk2295)* mutants, however, there was no discernable difference between primary siRNA levels in the oxidized and non-oxidized libraries, indicating that the 3′ modification on these small RNAs is lost in *henn-1* mutants (Figure S4).

henn-1 promotes germline RNAi for reasons unknown, although its role in somatic RNAi is confounded by its effect on the ERGO-1-class 26G-RNA pathway, which, when disrupted, enhances RNAi and could, thus, counter modest RNAi defects (Billi et al., 2012; Kamminga et al., 2012; Yigit et al., 2006). Our results indicating that exogenous primary siRNAs are methylated may explain why *henn-1* mutants are partially RNAi-defective in the germline. It is possible, however, that the reduction in *sid-1* and *rde-11* mRNA levels we identified by RNA-seq also contributes to the reduced RNAi sensitivity of *henn-1* mutants, as these genes are also required for optimal RNAi (Winston et al., 2002; Yang et al., 2012; Zhang et al., 2012). Our results also demonstrate that each

class of small RNAs that acts upstream of the WAGO-class 22G-RNA pathway contains a *henn-1*-dependent 3′ modification. Because HENN-1 is a 3′ methyltransferase, these results suggest that methylation is uniquely associated with primary small RNAs.

Subpopulations of miRNAs Contain 3′-End Modifications. In addition to binding primary siRNAs during RNAi, RDE-1 interacts with miRNAs (Corrêa et al., 2010). miRNAs are not generally methylated in *C. elegans* (Billi et al., 2012; Kamminga et al., 2012; Montgomery et al., 2012), but given our data suggesting that primary siRNAs, which bind RDE-1, are methylated, we tested whether a subset of miRNAs, particularly those bound by RDE-1, might also be methylated. To individually assess miRNA 3′-end modifications, we sequenced small RNAs from wild-type animals after treating the RNA with the oxidizing agent sodium periodate or a control. Consistent with previous studies, piRNAs and ERGO-1-class 26G-RNAs were enriched in libraries prepared from oxidized small RNAs, indicating that they are modified at their 3′ ends (Figure 2.5A) (Billi et al., 2012; Kamminga et al., 2012; Montgomery et al., 2012; Ruby et al., 2006; Vasale et al., 2010). Other classes of small RNAs were largely depleted in the oxidized libraries, although a subset of WAGO-class 22G-RNAs was also modestly enriched, which we did not explore further (Figure 2.5A). Six small RNAs annotated as miRNAs were enriched in libraries from oxidized small RNAs (Figure 2.5A). Upon closer inspection, two of these small RNAs, miR-78 and miR-4936, bear hallmarks of piRNAs—21 nt long, contain a 5′ U, and are depleted in *prg-1* mutants (Phillips et al., 2015)—suggesting that they are misannotated. Hence, we identified four high-confidence miRNAs, namely, miR-232-5p, miR-240-5p, miR-789, and miR-4814-3p, that were enriched by oxidation and are, therefore, modified at their 3′ ends. Each of these

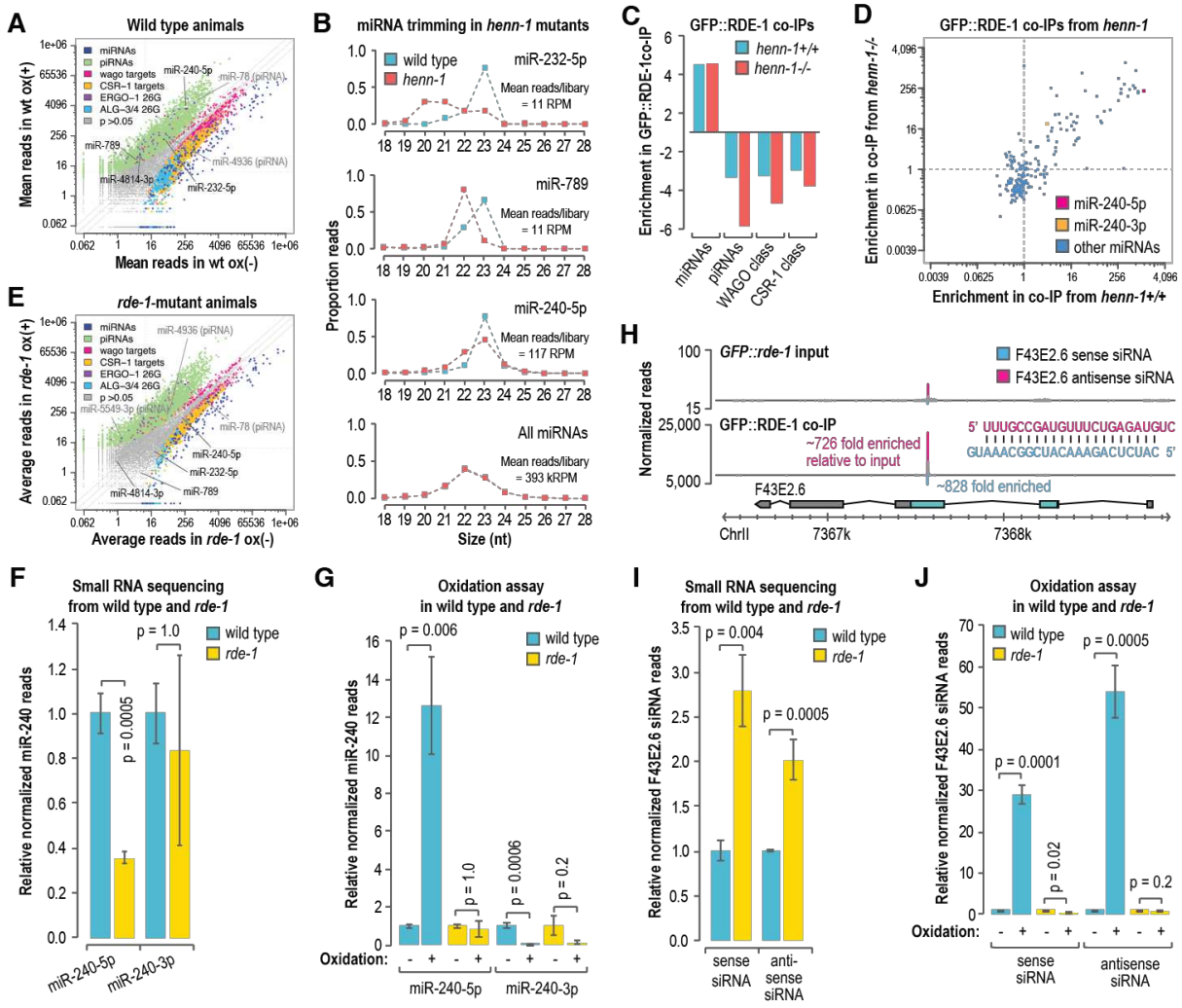

Figure 2.5. Accumulation of Modified miRNAs and Primary siRNAs Is Dependent on *rde-1* (A) Scatterplot displaying each small RNA feature (miRNA, piRNA, WAGO-class 22G-RNA locus, CSR-1-class 22G-RNA locus, ALG-3/4-class 26G-RNA locus, and ERGO-1-class 26G-RNA locus) as the average number of normalized reads in control (x axis, ox−) and oxidized small RNA libraries (y axis, ox+) (n = 3 biological replicates). Data are from wild-type L4-stage animals. (B) The proportions of total reads for each miRNA in L4 larvae are plotted by size. The “all miRNAs” plot corresponds to the combined proportions of reads for all annotated miRNAs. The data do not contain biological replicates. (C) Enrichment or depletion of the indicated classes of small RNAs in GFP::FLAG::RDE-1 coIPs relative to cell lysates. Data are shown for 1 of 2 biological replicates. (D) Scatterplot displaying each miRNA as its enrichment in GFP::FLAG::RDE-1 coIPs relative to cell lysates from adult animals wild type (*henn-1+/+*) (x axis) or mutant for *henn-1* (*henn-1(pk2295)*) (y axis). Dashed lines are at 1-fold enrichment on each axis. (E) Scatterplot displaying each small RNA feature, as in (A), as the average number of normalized reads in control (x axis, ox−) and oxidized small libraries (y axis, ox+) (n = 3 biological replicates). Data are from *rde-1(ne219)* L4-stage

animals grown in parallel to the wild-type animals used in (A). (F) miR-240-5p and miR-240-3p reads in *rde-1(ne219)* relative to wild type (n = 3 biological replicates). Error bars report standard deviation. (G) miR-240-5p and miR-240-3p reads in wild type and *rde-1(ne219)* from small RNA libraries treated with sodium periodate (oxidation +) relative to libraries receiving a control treatment (oxidation −) (n = 3 biological replicates). Error bars report standard deviation. (H) Read distribution across the F43E2.6 siRNA-generating locus from *GFP::FLAG::rde-1* cell lysate (input, top plot) and GFP::FLAG::RDE-1 coIP small RNA libraries (bottom plot). The most abundant siRNA duplex produced from the locus is shown. Enrichment in the GFP::FLAG::RDE-1 coIP relative to the input is shown for each siRNA. (I) F43E2.6 sense and antisense siRNA reads in *rde-1(ne219)* relative to wild type (n = 3 biological replicates). Error bars report standard deviation. (J) F43E2.6 sense and antisense siRNA reads in wild type and *rde-1(ne219)* from small RNA libraries treated with sodium periodate (oxidation +) relative to libraries receiving a control treatment (oxidation −) (n = 3 biological replicates). Error bars report standard deviation.

miRNAs was previously shown to interact with RDE-1 (Corrêa et al., 2010). Three of the four miRNAs enriched by oxidation in wild-type animals were truncated in *henn-1* mutants, indicating that *henn-1* protects them from 3′ trimming and is, thus, likely responsible for modifying their 3′ ends (Figure 2.5B). The levels of the fourth miRNA miR-4814-3p did not pass our read threshold (10 reads per million total) in our wild-type and *henn-1(pk2295)* set of libraries and was not analyzed. These data suggest that a subset of miRNAs is modified at their 3′ ends, and because this modification requires *henn-1*, we conclude that they are likely methylated.

miRNA and Primary siRNA 3′ Modifications Are Dependent on *rde-1.* To determine if RDE-1 could have a role in promoting small RNA methylation or, alternatively, if small RNA methylation might promote RDE-1 association, we first coIP'd RDE-1 from a strain in which a GFP::FLAG cassette was integrated into the endogenous *rde-1* locus using CRISPR-Cas9. Consistent with a previous study in which RDE-1 was coIP'd from an overexpression line, GFP::FLAG::RDE-1 predominantly associated with miRNAs (Figure 5C) (Corrêa et al., 2010). miRNA association with RDE-1 was not dependent on methylation, as GFP::FLAG::RDE-1 largely bound the same miRNAs in both wild-type and *henn-1(pk2295)* mutants (Figure 2.5D).

We next tested whether miRNA 3′ modifications are dependent on *rde-1*. In parallel to the wild-type animals described above (Figure 2.5A), we sequenced oxidized and non-oxidized small RNAs from *rde-1(ne219)* mutants. Unlike in wild-type animals, we did not identify any authentic miRNAs that were enriched by oxidation in *rde-1(ne219)* mutants; however, piRNAs, which also contain a *henn-1*-dependent 3′ modification were enriched, indicating that the loss of miRNA modifications is not due to *henn-1*

dysfunction in *rde-1* mutants (Figure 2.5E). Of the four miRNAs enriched by oxidation in our wild-type small RNA sequencing libraries, miR-240-5p was the most strongly enriched in our GFP::FLAG::RDE-1 coIP from *henn-1*+/+ animals (~1,226-fold) (Figure 2.5D). miR-240-5p levels were reduced by ~70% in *rde-1* mutants ($p = 0.0005$), which suggests that RDE-1 is its primary binding partner and that it is destabilized in its absence (Figure 2.5F). In wild-type libraries prepared from oxidized small RNAs, miR-240-5p was enriched ~12-fold relative to non-oxidized small RNA libraries ($p = 0.006$) (Figure 2.5G). In contrast, miR-240-5p was not enriched by oxidation in *rde-1* mutant libraries ($p = 1.0$) (Figure 2.5G). miR-240-3p, which is produced from the same precursor as miR-240-5p but from the opposite arm of the miRNA duplex, was only modestly enriched in our GFP::FLAG::RDE-1 coIP from *henn-1*+/+ animals (~4-fold) (Figure 2.5D). We were not able to detect a difference in miR-240-3p levels in *rde-1* mutants (Figure 2.5F). miR-240-3p was not enriched in oxidized small RNA libraries from either wild-type or *rde-1* mutants, indicating that despite being processed from the same duplex as miR-240-5p, it is not modified at its 3′ end (Figure 2.5G). Thus, miR-240-5p, a presumably strong RDE-1 interactor, is enriched by oxidation and, therefore, contains a 3′ modification, whereas miR-240-3p, a relatively weak RDE-1 interactor, is not modified. miR-240-3p also associates with ALG-1 and ALG-2 and miR-240-5p associates with ALG-5, suggesting that the fractions of miR-240 that we detected in *rde-1* mutants are likely associated with other Argonautes in an unmethylated form (Brown et al., 2017).

Endogenous canonical siRNAs resembling those produced from exogenous dsRNA are also predicted to bind RDE-1. Indeed, we identified endogenous siRNAs produced

from the F43E2.6 gene locus that were strongly enriched in our GFP::FLAG::RDE-1 coIPs (Figure 2.5H). F43E2.6 siRNAs were produced from a duplex that is 23 nt long and has 2-nt 3′ overhangs, indicating that it is likely processed by Dicer and is, therefore, a canonical siRNA locus (Figure 2.5H) (Ameres and Zamore, 2013; Warf et al., 2012). Furthermore, the levels of F43E2.6 siRNAs were elevated in mut-16 mutants, indicating that they are not produced through the Mutator pathway, unlike WAGO-class 22G-RNAs (Figure S5A) (Phillips et al., 2012; Zhang et al., 2011). F43E2.6 siRNAs were modestly elevated in *rde-1* mutants ($p \leq 0.004$), suggesting that association with RDE-1 destabilizes them relative to other Argonautes they might interact with or that their production is elevated in the absence of *rde-1* (Figure 2.5I). Both sense and antisense F43E2.6 siRNAs were enriched in GFP::FLAG::ALG-1 coIPs, indicating that they are partitioned between at least two Argonautes (Figure S5B) (Brown et al., 2017). In wild-type samples, the F43E2.6 sense strand siRNA was enriched by ~30-fold and the antisense siRNA by ~55-fold in oxidized small RNA libraries relative to non-oxidized small libraries, indicating that both strands of the duplex contain a 3′ modification ($p \leq 0.0005$) (Figure 2.5J). Conversely, neither siRNA was enriched in oxidized small RNA libraries from *rde-1* mutants, suggesting that accumulation of these siRNAs in their 3′ modified form is dependent on their association with RDE-1 (Figure 2.5J). These results point to a link between RDE-1 association and miRNA and primary siRNA 3′ modification, a modification dependent on *henn-1* and, therefore, likely methylation, and thus, we speculate that RDE-1 may direct small RNA methylation.

Discussion. The germline mortality of *henn-1* mutants likely relates to its role in the piRNA pathway, as disrupting the other small RNA pathways that *henn-1* is implicated

in, those involving the Argonautes ERGO-1 and RDE-1, does not result in progressive sterility (Figures S1C and S1D) (Sakaguchi et al., 2014). The progressive sterility of *henn-1* mutants follows a similar, albeit temperature sensitive, progression to that of *prg-1*/piwi mutants (Simon et al., 2014). Immediate sterility ensues after reestablishing the WAGO pathway, and therefore endogenous RNAi, in the absence of maternal *henn-1* or *prg-1* (de Albuquerque et al., 2015; Phillips et al., 2015). Animals heterozygous for *henn-1* in which the wild-type copy of the gene was contributed by the father, which presumably becomes active at the maternal-to-zygotic transition that occurs at the ~28-cell stage, displayed equal rates of sterility to animals homozygous mutant for *henn-1* after reestablishing endogenous RNAi. Thus, a model emerges in which maternally inherited methylated piRNAs and/or *henn-1* establish proper RNA silencing during embryogenesis, which presumably persists throughout germline development to ultimately impact fertility. This would likely occur through the initiation of secondary WAGO-class 22G-RNA production, which is thought to provide a memory of piRNA activity (Ashe et al., 2012; Buckley et al., 2012; Luteijn et al., 2012; Shirayama et al., 2012). In support of this, we observed similar effects on 22G-RNA levels across development in *henn-1* mutants, despite *henn-1* only being required for piRNA stability in embryos and early larval stages (Billi et al., 2012).

Although *henn-1*, and by extension methylation, has an important role in germline proliferation, it appears to have little impact on piRNA stability in the adult germline. Why methylation is important for piRNA stability in embryos but not in adult germ cells is unclear. It is possible that the genes involved in piRNA decay in embryos are absent in adults; however, we saw a similar degree of piRNA trimming in wild-type embryos and

adults, suggesting there may be two distinct mechanisms for piRNA decay, only one of which is affected by methylation. Alternatively, methylation may be specifically required for stabilizing piRNAs during maternal deposition in the embryo. P granules, the germ granules that house PRG-1/Piwi, break away from nuclear envelope after fertilization, possibly releasing piRNAs into the cytoplasm, which may expose them to decay machinery that they are normally protected from in P granules (Seydoux, 2018). It is also possible that piRNAs engage a distinct set of targets in embryos to which they have extensive complementarity at their 3′ ends and as a consequence are more susceptible to target-directed decay. This would hint at a role for piRNAs in early development that is perhaps distinct from their role later in development. piRNA-mRNA interactions that require only partial complementarity, which is common in *C. elegans* (Shen et al., 2018; Zhang et al., 2018), may not be affected by methylation. Modulation of methylation may even promote one function of piRNAs over another, which could explain why genes misregulated in *henn-1* mutants, despite nearly all being potential piRNA targets, were not uniformly up- or downregulated.

Our results demonstrate that small RNAs that act upstream of the Mutator complex, the WAGO-class 22G-RNA amplification component of the RNAi pathway, contain a 3′ modification that is dependent on *henn-1* and, thus, presumably methylation, whereas those that do not act as primary small RNAs are not modified (Billi et al., 2012; Kamminga et al., 2012; Montgomery et al., 2012). The Mutator complex contains a nucleotidyltransferase (MUT-2) and a 3′–5′ exonuclease (MUT-7), both of which could promote decay of primary small RNAs that feed into the pathway (Phillips et al., 2012). It is possible that methylation protects primary small RNAs from degradation by the

RNAi machinery or by factors that bridge the primary and secondary small RNA pathways. In support of this model, in Arabidopsis, methylation protects small RNAs from uridylation by HESO1, which is recruited to mRNA targets by the Argonaute AGO1 to facilitate decay of the 5′ fragment generated by AGO1 cleavage (Wang et al., 2018).

We showed that *rde-1* is required for the accumulation of miRNAs and canonical siRNAs containing modifications at their 3′ ends. Although we identified only a small subset of miRNAs that were resistant to oxidation, an indicator of the presence of a 3′ modification, most miRNAs were enriched in our RDE-1 coIPs. Therefore, if RDE-1 directs small RNA methylation, subpopulations of most individual miRNAs are likely methylated. Methylated miRNAs bound to RDE-1 may have a distinct function from non-methylated miRNAs bound to the other miRNA-associated Argonautes, ALG-1, ALG-2, and ALG-5. miR-243, for example, promotes mRNA entry into the endogenous RNAi pathway through its association with RDE-1 (Corrêa et al., 2010). miR-243, however, was not enriched by oxidation possibly because it also binds strongly to ALG-1 (Brown et al., 2017). In Drosophila, miRNAs predominantly associate with Ago1 and are not methylated; however, some also associate with the predominantly siRNA-associated Argonaute Ago2 and are methylated, consistent with Drosophila Ago2 directing small RNA methylation (Ameres et al., 2010; Horwich et al., 2007). It seems an analogous system may exist in *C. elegans* between the miRNA-associated Argonaute ALG-1, ALG-2, and ALG-5 and the exogenous siRNA-Argonaute RDE-1. It was recently shown that miRNAs are methylated in sea anemones, which commonly interact with near-perfect complementarity to their targets (Modepalli et al., 2018). Together with these

studies, our results raise the possibility that some degree of miRNA methylation is common in animals.

Materials and Methods.

Experimental Model and Subject Details. The Key Resources Table contains all of the *C. elegans* strains used in this study. Hermaphroditic animals were grown on nematode growth medium and fed *E. coli* OP50, except where noted otherwise. Animals used in the experiments in Figures 1A-1B, 1F-1G, 4, S1A-S1C, S1E, and S4 were grown at 25°C. All other animals were grown at 20°C. The developmental stage at which the animals were analyzed is specified in the methods and figures.

Strain Generation. USC1080 [*rde-1*(cmp133[(gfp + loxP + 3xFLAG)::*rde-1*]) V] and USC988[mut-16(cmp41[mut-16::mCherry + loxP]) wago-1(cmp92[(GFP + loxP + 3xFLAG)::wago-1]) I] were generated by introducing a GFP::3xFLAG cassette at the 5' end of the endogenous *rde-1* or *wago-1* coding sequence using CRISPR-Cas9 genome editing (Arribere et al., 2014; Dickinson et al., 2015; Dickinson et al., 2013). The repair templates were amplified using primers listed in the Key Resources Table and introduced into the vector pDD282 (Addgene #66823) by isothermal assembly (Gibson et al., 2009). To protect the repair template from cleavage, a mutation of the PAM sequence was incorporated into one of the primers. The guide RNA plasmid was generated by ligating oligos containing the guide RNA sequence into BsaI-digested pRB1017 (Addgene #59936) (Dickinson et al., 2013). TAM18 [*henn-1(ram13[henn-1ko; mCherry::Flag-no-stop-codon]) III*] was also generated using CRISPR-Cas9 (Dickinson et al., 2013). The repair template was amplified with the primers listed in the Key Resources Table and introduced into SpeI and ClaI digested pJJR83 (Addgene

#75028). The guide RNA construct was generated with the NEBuilder kit (New England BioLabs, E2621) using the plasmid pDD162 (Addgene #47549) and the primers listed in the Key Resources Table. The entire *henn-1* coding sequence was replaced with an mCherry::3xFLAG cassette lacking a stop codon and thus does not express mCherry. TAM20 [*mut-16(pk710) I; henn-1(pk2295) III*], TAM21 [*mut-16(pk710) I; henn-1(ram13) III*], TAM22 [*henn-1(pk2295) III; mut-14(mg464) smut-1(tm1301) V*], and TAM23 [*henn-1(ram13) III; mut-14(mg464) smut-1(tm1301) V*] were generated using standard genetic methods.

Multigenerational Brood Size Assays. Worms were grown on a continuous supply of *E. coli* (OP50) and chunked to fresh plates at each new generation (every 2-3 days). Because animals lay eggs over multiple days, the number of generations is approximate. Brood size assays were performed by separating 15 L4 larvae per strain onto individual plates, removing their offspring twice per day, and recording the number removed until the animals were no longer laying eggs. P-values were calculated using Wilcoxon rank-sum tests.

Transgenerational Sterility Assays. Transgenerational sterility assays were modeled after the approach used by Simon et al. and Ahmed et al. (Ahmed and Hodgkin, 2000; Simon et al., 2014). Briefly, 10 independent lines per wild type, *henn-1(pk2295), prg-1(n4357),* and *ergo-1(tm1860)* strain were grown at 20˚C or 25˚C. 10 worms per line were transferred to new plates every generation (2-3 days at 25˚C or 3-4 days at 20˚C) for 30 generations, and fertility was recorded at each transfer. Animals producing any number of offspring were considered fertile, and all offspring were transferred from plates on which there were fewer than 10 viable progeny.

Reestablishing Endogenous RNAi. The RNAi pathway was restored in RNAi-defective mutants using the genetics approach illustrated in Figure 1C as described (Phillips et al., 2015). Individual F1 animals from each cross were genotyped to confirm heterozygosity of *smut-1(tm1301)*, indicating that the progeny were from a cross. Animals that were wild-type or homozygous mutant for *smut-1* were excluded from the analysis. P-values were calculated using two-sample t-tests.

Imaging. Animals were imaged on a Zeiss Axio Imager Z2 upright microscope after immobilization in 10-25 uM sodium azide on 1.5 Agarose pads on glass slides.

Gonad Dissections. Animals were grown to gravid adult stage at 20˚C for 68-70 hours after L1 synchronization and dissected by cutting posterior to the pharynx or anterior to the tail in egg buffer containing 10 mM levamisole. Extruded distal gonads were collected by mouth pipetting, transferred to 500 ul Trizol, and frozen at -80°C (Campbell and Updike, 2015). Because the gonads break at the arms, the samples did not include the proximal gonad arms, which contain mature oocytes and sperm.

RNA Isolation. Dissected gonads and whole animals were flash frozen in liquid nitrogen prior to RNA isolation. RNA was isolated using Trizol (Life Technologies) followed by two chloroform extractions. RNA was precipitated in isopropanol for 20 minutes at room temperature for whole animal samples and overnight at -80˚C in the presence of 20 ug glycogen for germline, input, and co-IP samples.

Quantitative Real-Time PCR. Quantitative real-time-PCR of small RNAs was done as described using TaqMan reagents and custom probes following the manufacturers recommendations (Billi et al., 2012; Montgomery et al., 2012). Ct values were captured using a Bio-Rad CF96 Real-Time PCR Detection System. Ct values were averaged

across three technical replicates. Mean relative 21U-RNA levels across 3 biological replicates were calculated using the 2^{-ddCt} method (Livak and Schmittgen, 2001). miR-35 levels were used for normalization. Two-sample t-tests were used to compare differences between samples. Bonferroni adjustments were applied to correct for multiple comparisons.

Small RNA Northern Blot. 10 ug total RNA from each sample was resolved on a 17% denaturing polyacrylamide gel, transferred to a Hybond-N+ membrane (GE Healthcare), and UV crosslinked. T4 polynucleotide kinase (NEB) was used to radiolabel an LNA oligonucleotide antisense to 21UR-1 with ^{32}P-ATP. The membrane was incubated with the probe overnight at 38˚C in PerfectHyb Plus Hybridization Buffer (Sigma) and washed 5 times in SSC/SDS buffer at 50˚C for 20 minutes each wash.

Small RNA-Seq Libraries. Small RNAs were size selected (~16-30 nt) on 17% polyacrylamide/urea gels. Small RNA treatment varied by library as indicated in Table S5. Oxidation to enrich for 3'-2'-O-methylated small RNAs was done using 200 mM sodium periodate in borate buffer (pH 8.6) as described, but without beta-elimination (Montgomery et al., 2012; Yu and Chen, 2010). Polyphosphatase treatment to reduce 5' di- and triphosphates to monophosphates was done using RNA 5' polyphosphatase (Illumina). High-throughput sequencing libraries were prepared as described (Brown et al., 2017) or using the NEBNext Multiplex Small RNA Library Prep Kit (Illumina) (Table S5). The 3' ligation was done at 16˚C for 18 hours to improve capture of methylated small RNAs. PCR amplicons were size selected on 10% polyacrylamide non-denaturing gels.

Small RNA-Seq Data Analysis. 16-30 nt small RNA sequences were parsed from the library adapters, filtered to exclude reads with >1 base having a Phred quality score <30 and mapped to the *C. elegans* genome (Wormbase release WS230) using CASHX v. 2.3 (Fahlgren et al., 2009). miRNAs, piRNAs, WAGO-class 22G-RNA loci, CSR-1-class 22G-RNA loci, ALG-3/4-class 26G-RNA loci, and ERGO-1-class 26G-RNA loci were classified as described (Phillips et al., 2015). Differential expression analysis, including fold change and p value calculations, was done using DESeq2 v. 1.18.1 with the Benjamin Hochberg multiple test correction applied (FDR = 0.05) (Love et al., 2014). All other p-values reported for small RNA sequencing data were calculated using two-sample t-tests. Custom Perl and Python scripts, R, and Excel were used for all other data analyses. Plots were drawn in R, Excel, BioVenn, and IGV (Hulsen et al., 2008; Thorvaldsdottir et al., 2013). Sequencing was done on an Illumina NextSeq 500.

RNA-Seq Libraries. Ribosomal RNA was depleted from total RNA using Ribo-Zero rRNA Removal Kit (Human/Mouse/Rat) (Illumina). rRNA depleted RNA was purified using the RNA Clean & Concentrator kit (Zymo Research). DNase treatment was done on the columns used for RNA purification. High-throughput sequencing libraries were prepared from purified rRNA-depleted RNA using NEBNext Ultra™ II Directional RNA Library Prep Kit (NEB). Most sequencing was done on an Illumina NextSeq 500 (High Output Kit, 75 cycles) (Table S5).

RNA-Seq Data Analysis. Adapters and low-quality bases were removed using Trimmomatic v. 0.35 (Bolger et al., 2014). Reads were mapped to the *C. elegans* genome (Wormbase release WS230) using Star v. 2.5.0a (Dobin et al., 2013). Reads from specific genes were counted using RSEM v. 1.3.0 (Li and Dewey, 2011).

Differential expression analysis, including fold change and p-value calculation, was done using DESeq2 v. 1.18.1 with the Benjamin Hochberg multiple test correction applied (FDR = 0.05) (Love et al., 2014). Plots were drawn with R and IGV (Thorvaldsdottir et al., 2013).

Transposon Analysis. To identify reads mapping to each annotated transposon family, mRNA and small RNA sequencing reads were aligned to each of 152 transposon family consensus sequences within using Bowtie (Langmead, 2010) (Jurka, 2000). Reads mapping to more than one transposon family were discarded. Differential expression analysis was done using DESeq2 v. 1.18.1 (Love et al., 2014).

RNAi Assays. Synchronized L1 larvae were transferred to *E. coli* HT115 containing an empty vector (L4440) or expressing dsRNA complementary to *pos-1* (Kamath et al., 2003) and grown at 25˚C. Gravid adults were collected for RNA isolation at 48 hours.

Co-Immunoprecipitations. FLAG::HRDE-1, GFP::FLAG::WAGO-1, and GFP::FLAG::RDE-1 were coimmunoprecipitated from gravid adults 68 hours after L1 synchronization. Animals were flash frozen in liquid nitrogen and lysed in 50 mM Tris-Cl, pH 7.4, 100 mM KCl, 2.5 mM $MgCl_2$, 0.1% Igepal CA-630, 0.5 mM PMSF, and 1X Pierce Protease Inhibitor Tablets. Cell lysates were cleared by centrifugation for 10 min at 12,000 RCF and incubated with anti-GFP mAb-agarose for 1 hour or with anti-FLAG followed by Protein G magnetic beads for a combination of 1 hour. After co-immunoprecipitation, beads were washed in lysis buffer and split into RNA and protein fractions. Antibody specificity for FLAG (FLAG::HRDE-1, GFP::FLAG::WAGO-1 co-IPs) or GFP (GFP::FLAG::RDE-1) was confirmed by doing negative control co-IPs from wild-type animals.

Quantification and Statistical Analysis. The statistical tests used are described within the methods section describing each experiment. Bonferroni multiple test corrections were applied to p-values when comparing >2 conditions. All error bars report standard deviation.

Data and Software Availability. All the high-throughput sequencing data described here has been deposited to the Gene Expression Omnibus (GEO) and is available under accession number GSE137734. Software used in the study is described in the corresponding methods section. Custom R, Perl, and Python scripts are available on request.

Table 1: Key Resources Table

Reagent or Resource	Source	Identifier
Antibodies		
anti-GFP mAb-agarose	MBL	Cat# D153-8; RRID:AB_591815
anti-FLAG	Sigma	Cat# F1804; RRID:AB_262044
Bacterial Strains		
E. coli OP50	Gary Ruvkun (Harvard Medical School)	N/A
E. coli HT115	Gary Ruvkun (Harvard Medical School) (Kamath et al., 2003)	N/A
Chemicals, Peptides, and Recombinant Proteins		
Trizol	Life Technologies	15596018
RNA 5′ polyphosphatase	Illumina	RP8092H
NEBNext 2X PCR Master Mix	NEB	M0541L
TURBO DNase	Life Technologies	AM2238
AMPure XP Beads	Beckman Coulter	A63881
Pierce Protease Inhibitor Tablets	Pierce Biotechnology	88266

Amersham Hybond -N+ Membranes	GE Healthcare	RPN303B
PerfectHyb Plus Hybridization Buffer	Sigma-Aldrich	H7033
T4 Polynucleotide Kinase (3′ phosphatase minus)	NEB	M0236S
SureBeads Protein G Magnetic Beads	Bio-Rad	161-4023
Critical Commercial Assays		
TaqMan	Life Technologies	4366596, 4444557, 4427975
NEBNext Ultra II Directional RNA Library Prep Kit for Illumina	NEB	E7760S
RNA Clean & Concentrator	Zymo Research	R1015
Ribo-Zero rRNA Removal Kit (Human/Mouse/Rat)	Illumina	MRZH11124
NEBNext Small RNA Library Prep Kit for Illumina	NEB	E7300S or E7580S
Deposited Data		
NGS data	This Study	Gene Expression Omnibus GSE137734
Experimental Models: Organisms/Strains		

C. elegans Bristol Strain	CGC	N2
glp-4(bn2) I	CGC	SS104
henn-1(pk2295) III	René Ketting (IMB Mainz)	NL4415
prg-1(n4357) I	CGC	SX922
rde-1(ne219) V	CGC	WM27
mut-14(mg464) smut-1(tm1301) V	Phillips et al., 2015	GR1948
mut-16(pk710) I	*CGC*	NL1810
henn-1(pk2452) III	René Ketting (IMB Mainz)	RFK30
glh-1(sam24[glh-1::gfp::3Xflag]) I	Dustin Updike (MDI)	DUP64
glh-1(sam24[glh-1::gfp::3Xflag]) I; henn-1(pk2295) III	This Study	TAM56
rde-1(cmp133[(gfp + loxP + 3xFLAG)::rde-1]) V	This Study	USC1080
mut-16(cmp41[mut-16::mCherry + loxP]) wago-1(cmp92[(GFP + loxP + 3xFLAG)::wago-1]) I	This Study	USC988
henn-1(ram13[henn-1ko; mCherry::Flag-no-stop-codon]) III	This Study	TAM18

mut-16(pk710) I; henn-1(pk2295) III	This Study	TAM26
mut-16(pk710) I; henn-1(ram13) III	This Study	TAM36
henn-1(pk2295) III; mut-14(mg464) smut-1(tm1301) V	This Study	TAM27
henn-1(ram13) III; mut-14(mg464) smut-1(tm1301) V	This Study	TAM35
flag::hrde-1([flag::hrde-1, cb-unc-119(+)]) II; unc-119(ed3) III	Craig Mello (University of Massachusetts) (Shirayama et al., 2012)	N/A
Oligonucleotides		
See Table S5	See Table S5	N/A
Recombinant DNA		
pDD282 (GFP::3xFLAG repair template plasmid)	Addgene (Dickinson et al., 2015)	66823
pRB1017 (Guide RNA plasmid)	Addgene (Arribere et al., 2014)	59936
pJJR83 (mCherry::3xFLAG repair template plasmid)	Addgene (a gift from Mike Boxem)	75028
pDD162 (Guide RNA	Addgene (Dickinson et al.,	47549

plasmid)	2013)	
L4440 (RNAi vector)	Addgene (a gift from Andrew Fire)	1654
pos-1 RNAi plasmid	Gary Ruvkun (Harvard Medical School) (Kamath et al., 2003)	N/A
Software and Algorithms		
CASHX v. 2.3	Fahlgren et al., 2009	N/A
DESeq2 v. 1.18.1	Love et al., 2014	https://bioconductor.org/packages/release/bioc/html/DESeq2.html
Trimmomatic v. 0.35	Bolger et al., 2014	http://www.usadellab.org/cms/?page=trimmomatic
Star v. 2.5.0a	Dobin et al., 2013	https://github.com/alexdobin/STAR
Bowtie	Langmead, 2010	http://bowtie-bio.sourceforge.net/index.shtml
RSEM v. 1.3.0	Li and Dewey, 2011	https://deweylab.github.io/RSEM/
Zen Image Analysis	Zeiss	N/A

Author Contributions and Acknowledgements for Svendsen et al., 2019.

Experiments were conceptualized by Tai Montgomery and Joshua Svendsen. Experiments were performed by Tarah Vijayasarathy, Rachel Tucci, Brooke Montgomery, Tai Montgomery, Kristen Brown, and Joshua Svendsen. More specifically, Rachel performed RNAi reset crosses, genetic screens; Tarah performed RNAi reset crosses; Tai performed *henn-1* germline imaging, northern blots, immunoprecipitation; Brooke performed qPCR, Small RNA sequencing library prep, mRNA sequencing library prep, genetic screens; Kristen performed gonad isolation**;** Joshua performed progressive sterility assays and brood size assays, qPCR, mRNA sequencing library prep, small RNA sequencing library prep, gonad isolation, immunoprecipitation. High throughput sequencing was performed by Justin Lee, Marylee Layton, the Anschutz Genomics and Microarray Core, and Novogene. High throughput sequencing data were analyzed by Tai Montgomery and Kailee Reed. Paper was written by Tai Montgomery and Joshua Svendsen. Figures were created by Tai Montgomery, Kailee Reed, and Joshua Svendsen. Strains were provided by Carolyn Phillips, Rene Ketting, Dustin Updike, Craig Mello, and the Caenorhabditis Genetics Center. CRISPR strains were generated by Taylor Marks, Carolyn Philips, and Dieu An Nguyen. Gonad isolation methods were conceptualized by Dustin Updike and adapted by Kristen Brown and Joshua Svendsen.

CHAPTER 3: Conclusions, Implications, and Future Directions.

In summary of my thesis work, I identified a role for small RNA methylation in maintaining *C. elegans* germline immortality, characterized the classes of small RNAs that are methylated, and identified factors that influence which small RNAs are methylated. Additionally, I synthesized recent advances in the field of piRNA biology and their potential impacts on future research.

The Progressive Sterility Phenotype of *henn-1* is due to Loss of piRNA Modification. Our results demonstrate a requirement for piRNA methylation, but not the methylation of other small RNAs, in maintaining germline integrity. A recent study on progressive sterility in piRNA mutants provides a possible mechanism underlying this phenotype by showing that that the progressive sterility associated with piRNA loss is due to deregulation of histone genes. When the Mutator-associated secondary siRNA pathway is not directed against targets identified by piRNAs, it is instead capable of silencing histone genes, resulting in reduced availability of histones for incorporation into chromatin and, eventually, germline mortality (Barucci et al., 2020). This conclusion is supported by our own observation that histone genes are downregulated in piRNA mutant germlines, and by observations made in another recent paper from our lab (Reed et al. 2020). If loss of methylation leads to piRNA destabilization, maintenance of histone expression is likely also methylation dependent.

We have also observed that germline mortality is not a phenotype associated with loss of the Mutator complex and the WAGO-class 22G-RNAs it produces. Since the only known function of piRNAs in *C. elegans* is to initiate RNAi, this suggests that future

efforts to understand the full functionality of piRNAs should look beyond their well-characterized participation in the Mutator-dependent RNAi pathway. Further, our observation that loss of primary small RNA methylation has only a modest effect on WAGO-class 22G-RNA production but severe impacts on fertility and germline integrity suggests that any Mutator-independent functions of piRNAs could be dependent on methylation by *henn-1*. It may be valuable to determine whether the progressive sterility we observe in piRNA mutants is actually a distinct phenotype from those observed in Mutator mutants. Since piRNAs are responsible for initiating the RNA silencing maintained by WAGO-class 22G-RNAs, it is possible that, without the guidance of piRNAs, essential genes become targeted by the Mutator pathway over the course of many generations. Previous work suggests that, in the absence of piRNAs, resetting the memory of RNAi conferred by 22G-RNAs results in immediate sterility due to the misrouting of essential genes into the RNAi pathway (Phillips et al., 2015). If 22G-RNAs are unable to maintain correct gene silencing programs alone, the prolonged absence of piRNAs as a means of distinguishing non-self genetic elements could result in degradation of the germline's genome over time. This possibility could be tested by isolating RNA from piRNA deficient mutants, methylation deficient mutants, and Mutator mutants at several timepoints and looking for either misregulated genes or changes in small RNA profiles. If this possibility is tested and ruled out, such a result may point to a function of piRNAs that is completely Mutator-independent. It is also possible that Mutator mutants do not become progressively sterile because they are not silencing histones like they do in piRNA mutants (Barucci et al., 2020), or it may be a combination of the two.

piRNA Methylation is Required in Embryos, but not the Adult Germline. The results of our study imply a role for methylation in stabilizing piRNAs during early development. The reason they need to be stabilized at this point but not in the adult germline, however, remains unclear. As we speculate earlier in the paper, it is possible that maternal piRNAs require protection while being deposited into the oocytes, that piRNAs are exposed to decay machinery when the P-granule separates from the nuclear envelope at fertilization, or that piRNAs have roles in the embryo that are distinct from their roles in the developed germline. A logical starting point for answering these questions would be to measure piRNA levels in *henn-1* mutant embryos at several points in embryogenesis to determine whether there is a point at which methylation stops being necessary. If a specific window during which methylation is protective can be identified, closer examinations of the coincident processes governing RNA metabolism could reveal which one is responsible for turning over piRNAs. The specific piRNAs that are present in the embryo could also be examined to determine whether different genes are targeted at that stage than are targeted in the adult germline, and whether target selection affects piRNA stability as it does in *Drosophila* (Horwich et al., 2007). The difficulty in this approach is gathering enough RNA to perform the analysis. We attempted stage-specific embryo collection by dissecting gravid adult animals and collecting the embryos by hand, but we were consistently unable to recover detectable levels of RNA after extraction. Given the labor-intensive nature of this type of sample collection, it may be wise to explore more efficient methods such as flow cytometry to separate embryos of different stages for analysis. I personally believe that it is a question worth pursuing, as identifying the point or points at which

piRNAs are degraded would be helpful in answering not only the question of why piRNAs require methylation at different developmental stages, but could also narrow the search for the piRNA turnover machinery.

RDE-1 Directs Methylation of Small RNAs. In other organisms like Drosophila, the Argonaute protein into which a small RNA is loaded determines whether it will be methylated (Ameres et al. 2010; Horwich et al. 2007). Our results suggest that this is true in *C. elegans* as well. We have not, however, been able to detect a stable interaction between HENN-1 and an Argonaute protein. Like previous attempts made with PRG-1 by Kamminga et al. (2012), our attempts to co-IP HENN-1 and RDE-1 were unsuccessful, meaning that the only meaningful insight we have into the interaction between these proteins is that it is not stable enough to survive immunoprecipitation, if it occurs at all. The aforementioned study did, however, find evidence that HENN-1 may oligomerize with another protein whose identity remains unknown. It is possible that this unidentified protein facilitates transient interactions between HENN-1 and Argonaute proteins or, even more interestingly, is involved in the decay of unmethylated small RNAs. Should future efforts be directed toward understanding the specific biochemical mechanism of small RNA methylation in *C. elegans*, mass spectrometry could be helpful in identifying this and any other hypothetical binding partners with which HENN-1 associates. Although our lab currently lacks the expertise to use mass spec in this way, the Ketting lab at IMB Mainz uses this technique to identify protein participants in the *C. elegans* RNAi pathway (Almeida et al. 2018).

A Subpopulation of miRNAs is Methylated. Although plant miRNAs are commonly methylated, animal miRNAs are not. Our results indicate that a subpopulation of *C.*

elegans miRNAs is methylated. We do not yet understand what functions these miRNAs perform and how methylation affects them, but knowing which argonaute they bind will make these questions easier to answer. For example, the miRNA miR-243 binds to RDE-1 and, unlike any other miRNA observed in *C. elegans*, triggers the entry of its targets into the secondary small RNA biogenesis pathway (Corrêa et al. 2010). Although this miRNA was not enriched by oxidation in our hands, possibly because it also associates with ALG-1 (Brown et al. 2017), it suggests that at least some RDE-1-associated miRNAs may perform functions that other miRNAs do not. Interestingly, our data show that the majority of miRNAs associate to some degree with RDE-1, suggesting that a subpopulation of most miRNAs is methylated. Obviously, these results raise questions about how RDE-1 fits into the larger landscape of miRNA-mediated gene regulation. Previous work from our lab indicates that the miRNA-associated Argonoutes of *C. elegans* display functional specialization (Brown et al., 2017), so it would not be unreasonable to hypothesize that RDE-1 and its methylated miRNAs fill a functional niche that the other miRNA-associated Argonautes are unable to cover. Examining miRNA-associated phenotypes in *rde-1* mutants or methylation deficient mutants could point to functions that miRNAs may need to be methylated to perform. RDE-1-associated (and thus methylated) miRNAs have not been thoroughly investigated, but the work that has been done on miR-243, an RDE-1 associated miRNA, indicates that it initiates secondary siRNA production (Correa et al., 2010). Currently, miR-243 is the only known *C. elegans* miRNA that does this, but the possibility that other methylated miRNAs handle their targets similarly remains to be examined. In sea anemones, another animal in which some miRNAs are methylated,

methylation protects miRNAs that share perfect complementarity with their targets (Modepalli et al., 2018). While our study has not shown perfect complementarity to be a reliable determinant of small RNA methylation in *C. elegans*, different classes of small RNAs may need to be methylated for different reasons, and miRNAs whose 3' ends are highly complementary to their targets may need additional protection in the form of methylation. Interestingly, a recent study on small RNA profiling in the germline indicates that primary small RNA machinery that responds to environmental dsRNA is expressed at the same level in both germline sexes, but secondary small RNA biogenesis machinery is expressed in lower levels in males (Bezler et al., 2019). In this case, miRNAs could associate with RDE-1 as a means of regulating which miRNAs are expressed in which germline, and the lack of Mutator proteins in the male germline may bias RDE-1 toward miRNA-related rather than RNAi-related functions.

RDE-1 Interacts with at Least One Endogenous Canonical siRNA. Although RDE-1 is primarily known for its role in facilitating exogenous RNAi by binding to exogenous siRNAs, it also appears to participate in endogenous RNAi pathways. In our study, we found that RDE-1 binds to at least one endogenous canonical siRNA derived from the F43E2.6 locus. Since endogenous canonical siRNAs are uncommon in *C. elegans*, the identification of an additional Argonaute capable of binding them could provide a means of investigating additional biological processes these siRNAs participate in. Additionally, since this Argonaute promotes small RNA methylation, enriching for methylated small RNAs may be a method of identifying more of these canonical siRNAs.

The Purpose of Small RNA Methylation in *C. elegans* Remains Unknown. One of the first observations we made about small RNA methylation when this study began

was that the small RNAs that function upstream of the Mutator pathway, the primary small RNAs, are methylated at their 3' end. This observation was supported by our results indicating that exogenous siRNAs bound by RDE-1 are methylated. We did not, however, identify a specific mechanistic reason primary small RNAs need to be methylated. The degree of complementarity between a small RNA and its target does not appear to influence which small RNAs are methylated in *C. elegans,* suggesting that small RNA methylation serves a purpose in worms that has not already been identified in other organisms. One such possible function is protecting piRNAs that bind to mRNAs and sequester them in the P granules of germ cells. Surviving extended periods of target engagement may require that piRNAs be methylated, a task that has little to do with how much complementarity the piRNA shares with its target. One way to test whether methylation contributes to this function would be to introduce *rde-11* and *sid-1* mutations (both of which are genes that piRNAs sequester in P granules) into *henn-1* mutants and measuring whether there is a change in the stability of piRNAs predicted to bind those genes (Ouyang et al. 2019).

Since the Mutator complex contains a number of RNA-metabolizing enzymes, it is also possible that methylation protects primary small RNAs as they engage their targets and shuttle them into the Mutator foci. Since, in other organisms, methylation protects against degradation preceded by polyuridylation, the small RNAs that feed into the pathway may require protection from MUT-7 (a 3'-5' exonuclease) and MUT-2 (a nucleotidyltransferase that adds nontemplated Us). We tested this indirectly by measuring piRNA abundance in *henn-1* mutants both in the presence and absence of an additional mutation that prevents the nucleation of the Mutator complex by disabling

the Mutator protein MUT-16 (see Appendix 2 for more information). Our results showed no change in piRNA levels, but should by no means be considered conclusive. The *mut-16* mutation we introduced abolishes 22G-RNA formation, but we don't know whether the constituent proteins of the complex such as MUT-2 and MUT-7 remain active even when they are not part of the functional mutator complex. Repeating this experiment in *henn-1;mut-7* mutants would be the most direct way to test this hypothesis, but generating the double mutant is complicated by the two genes' proximity on chromosome III. Repeating the experiment with double mutants would certainly be more informative should this question be approached again (and if the difficulty of generating the mutants could be surpassed, perhaps by CRISPR-Cas9).

Another potential way to understand why some *C. elegans* small RNAs are methylated would be to identify the decay machinery that turns over unmethylated small RNAs. We have worked on answering this question with little success, but our efforts have yielded a few interesting insights (see Appendix 2 for more detailed information). The primary gene of interest identified by these efforts was *pup-3*, an annotated poly(U) polymerase with no known function. Although this result was promising due to the presumption that polyuridylation precedes degradation in worms (as in other organisms and as shown by Kamminga et al., 2012), follow-up experiments using a null mutant for *pup-3* were unable to rescue the piRNA depletion associated with *henn-1* mutation. It is possible that *C. elegans* employs redundant poly(U) polymerases to mark small RNAs for degradation like *Arabidopsis* does, but double mutants for other known poly(U) polymerases proved difficult to work with genetically (see Appendix 2). We recognize, however, that the assay we used to identify *pup-3* also comes with numerous caveats,

and that the evidence for U-tailing of *C. elegans* small RNAs is limited, so whether the gene we identified is involved in small RNA turnover at all remains inconclusive. Of all the questions we tried to answer over the course of this work, this is the one I find the most personally vexing, and I would be satisfied to see it answered. See Appendix 2 for more information on the efforts we have devoted to this question already and suggestions about how to proceed.

REFERENCES

Ahmed, S., and Hodgkin, J. (2000). MRT-2 checkpoint protein is required for germline immortality and telomere replication in *C. elegans*. Nature 403, 159–164.

Almeida, M.V., Dietz, S., Redl, S., Karaulanov, E., Hildebrandt, A., Renz, C., Ulrich, H.D., Konig, J., Butter, F., Ketting, R.F. (2018). GTSF-1 is required for formation of a functional RNA-dependent RNA polymerase complex in *Caenorhabditis elegans.* EMBO J. 37, e99325

Ambros, V., Lee, R.C., Lavanway, A., Williams, P.T., and Jewell, D. (2003). MicroRNAs and other tiny endogenous RNAs in *C. elegans*. Curr. Biol. 13, 807–818.

Ameres, S.L., and Zamore, P.D. (2013). Diversifying microRNA sequence and function. Nat. Rev. Mol. Cell Biol. 14, 475–488.

Ameres, S.L., Horwich, M.D., Hung, J.H., Xu, J., Ghildiyal, M., Weng, Z., and Zamore, P.D. (2010). Target RNA-directed trimming and tailing of small silencing RNAs. Science 328, 1534–1539.

Andralojc, K.M., Campbell, A.C., Kelly, A.L., Terrey, M., Tanner, P.C., Gans, I.M., Senter-Zapata, M.J., Khokhar, E.S., and Updike, D.L. (2017). ELLI-1, a novel germline protein, modulates RNAi activity and P-granule accumulation in Caenorhabditis elegans. PLoS Genet. 13, e1006611.

Aoki, K., Moriguchi, H., Yoshioka, T., Okawa, K., and Tabara, H. (2007). In vitro analyses of the production and activity of secondary small interfering RNAs in *C. elegans*. EMBO J. 26, 5007–5019.

Arribere, J.A., Bell, R.T., Fu, B.X., Artiles, K.L., Hartman, P.S., and Fire, A.Z. (2014). Efficient marker-free recovery of custom genetic modifications with CRISPR/Cas9 in Caenorhabditis elegans. Genetics 198, 837–846.

Ashe, A., Sapetschnig, A., Weick, E.M., Mitchell, J., Bagijn, M.P., Cording, A.C., Doebley, A.L., Goldstein, L.D., Lehrbach, N.J., Le Pen, J., et al. (2012). piRNAs can trigger a multigenerational epigenetic memory in the germline of *C. elegans*. Cell 150, 88–99.

Bagijn, M.P., Goldstein, L.D., Sapetschnig, A., Weick, E.M., Bouasker, S., Lehrbach, N.J., Simard, M.J., and Miska, E.A. (2012). Function, targets, and evolution of Caenorhabditis elegans piRNAs. Science 337, 574–578.

Bartel, D.P. (2004). MicroRNAs: genomics, biogenesis, mechanism, and function. Cell 116, 281-297.

Bartel, D.P. (2009). MicroRNAs: target recognition and regulatory functions. Cell 136, 215–233.

Barucci, G., Cornes, E., Singh, M., Li, B., Ugolini, M., Samolygo, A., Didier, C., Dingli, F., Loew, D., Quarato, P., Cecere, G. (2020). Small-RNA-mediated transgenerational silencing of histone genes impairs fertility in piRNA mutants. Nature Cell Biology 22, 235-245.

Batista, P.J., Ruby, J.G., Claycomb, J.M., Chiang, R., Fahlgren, N., Kasschau, K.D., Chaves, D.A., Gu, W., Vasale, J.J., Duan, S., Conte, D., Luo, S., Schroth, G.P., Carrington, J.C., Bartel, D.P. ,and Mello, C.C. (2008). PRG-1 and 21U-RNAs Interact to Form the piRNA Complex Required for Fertility in *C. elegans*. Mol. Cell 31, 67-78.

Beanan, M.J., and Strome, S. (1992). Characterization of a germ-line proliferation mutation in *C. elegans*. Development 116, 755–766.

Bernstein, E., Caudy, A.A., Hammond, S.M., and Hannon, G.J. (2001). Role for a bidentate ribonuclease in the initiation step of RNA interference. Nature 409, 363–366.

Bezler A., Braukmann F., West S.M., Duplan, A., Conconi, R., Schutz, F., Gonczy, P., Piano, F., Gunsalus, K., Miska E.A., Keller, L. (2019). Tissue- and sex-specific small RNAomes reveal sex differences in response to the environment. PLoS Genet. 15, e1007905.

Billi, A.C., Alessi, A.F., Khivansara, V., Han, T., Freeberg, M., Mitani, S., and Kim, J.K. (2012). The Caenorhabditis elegans HEN1 ortholog, HENN-1, methylates and stabilizes select subclasses of germline small RNAs. PLoS Genet. 8, e1002617.

Billi, A.C., Fischer, S.E., and Kim, J.K. (2014). Endogenous RNAi pathways in *C. elegans*. WormBook, 1–49.

Bolger, A.M., Lohse, M., and Usadel, B. (2014). Trimmomatic: a flexible trimmer for Illumina sequence data. Bioinformatics 30, 2114–2120.

Brown, K.C., Svendsen, J.M., Tucci, R.M., Montgomery, B.E., and Montgomery, T.A. (2017). ALG-5 is a miRNA-associated Argonaute required for proper developmental timing in the Caenorhabditis elegans germline. Nucleic Acids Res. 45, 9093–9107.

Branon, T.C., Bosch, J.A., Sanchez, A.D., Udeshi, N.D., Svinkina, T., Carr, S.A., Feldman, J.L., Perrimon, N., and Ting, A.Y. (2018). Efficient proximity labeling in living cells and organisms with TurboID. Nature Biotechnology 36, 880-887.

Buckley, B.A., Burkhart, K.B., Gu, S.G., Spracklin, G., Kershner, A., Fritz, H., Kimble, J.,

Fire, A., and Kennedy, S. (2012). A nuclear Argonaute promotes multigenerational epigenetic inheritance and germline immortality. Nature 489, 447–451.

Campbell, A.C., and Updike, D.L. (2015). CSR-1 and P granules suppress sperm-specific transcription in the *C. elegans* germline. Development 142, 1745–1755.

Carthew, R. W., and Sontheimer, E. J. (2009). Origins and Mechanisms of miRNAs and siRNAs. Cell 136, 642-655.

Claycomb, J.M., Batista, P.J., Pang, K.M., Gu, W., Vasale, J.J., van Wolfswinkel, J.C., Chaves, D.A., Shirayama, M., Mitani, S., Ketting, R.F., et al. (2009). The Argonaute CSR-1 and its 22G-RNA cofactors are required for holocentric chromosome segregation. Cell 139, 123–134.

Claycomb, J.M. (2014). Ancient endo-siRNA pathways reveal new tricks. Current Biology 24, R703-R715.

Correa, R.L., Steiner, F.A., Berezikov, E., and Ketting, R.F. (2010). MicroRNA-directed siRNA biogenesis in Caenorhabditis elegans. PLoS Genet. 6, e1000903.

de Albuquerque, B.F., Placentino, M., and Ketting, R.F. (2015). Maternal piRNAs Are Essential for Germline Development following De Novo Establishment of Endo-siRNAs in Caenorhabditis elegans. Dev. Cell 34, 448–456.

Dickinson, D.J., Ward, J.D., Reiner, D.J., and Goldstein, B. (2013). Engineering the Caenorhabditis elegans genome using Cas9-triggered homologous recombination. Nat. Methods 10, 1028–1034.

Dickinson, D.J., Pani, A.M., Heppert, J.K., Higgins, C.D., and Goldstein, B. (2015). Streamlined Genome Engineering with a Self-Excising Drug Selection Cassette. Genetics 200, 1035–1049.

Dobin, A., Davis, C.A., Schlesinger, F., Drenkow, J., Zaleski, C., Jha, S., Batut, P., Chaisson, M., and Gingeras, T.R. (2013). STAR: ultrafast universal RNA-seq aligner. Bioinformatics 29, 15–21.

Fahlgren, N., Sullivan, C.M., Kasschau, K.D., Chapman, E.J., Cumbie, J.S., Montgomery, T.A., Gilbert, S.D., Dasenko, M., Backman, T.W., Givan, S.A., and Carrington, J.C. (2009). Computational and analytical framework for small RNA profiling by high-throughput sequencing. RNA 15, 992–1002.

Fischer S.E.J., Montgomery T.A., Zhang C, Fahlgren N., Breen P.C., Hwang A., Sullivan C.M., Carrington J.C., Ruvkun, G. (2011) The ERI-6/7 helicase acts at the first stage of an siRNA amplification pathway that targets recent gene duplications. PLoS Genet. 7, e1002369.

Frøkjær-Jensen, C., Jain, N., Hansen, L., Davis, M.W., Li, Y., Zhao, D., Rebora, K., Millet, J.R.M., Liu, X., Kim, S.K., et al. (2016). An abundant class of non-coding DNA can prevent stochastic gene silencing in the *C. elegans* germline. Cell 166, 343–357.

Gibson, D.G., Young, L., Chuang, R.Y., Venter, J.C., Hutchison, C.A., III, and Smith, H.O. (2009). Enzymatic assembly of DNA molecules up to several hundred kilobases. Nat. Methods 6, 343–345.

Gent, J.I., Lamm, A.T., Pavelec, D.M., Mainar, J.M., Parameswaran, P., Tao, L., Kennedy S., and Fire, A.Z. (2010). Distinct phases of siRNA synthesis in an endogenous RNAi pathway in the *C. elegans* soma. Molecular Cell 37, 1-11.

Gou, L.T., Dai, P., Yang, J.H., Xue, Y., Hu, Y.P., Zhou, Y., Kang, J.Y., Wang, X., Li, H., Hua, M.M., et al. (2014). Pachytene piRNAs instruct massive mRNA elimination during late spermiogenesis. Cell Res. 24, 680–700.

Gu, W., Shirayama, M., Conte, D., Jr., Vasale, J., Batista, P.J., Claycomb, J.M., Moresco, J.J., Youngman, E.M., Keys, J., Stoltz, M.J., et al. (2009). Distinct argonaute-mediated 22G-RNA pathways direct genome surveillance in the *C. elegans* germline. Mol. Cell 36, 231–244.

Han, T., Manoharan, A.P., Harkins T.T., Bouffard, P., Fitzpatrick, C., Chu, D.S., Thierry-Mieg, D., Thierry-Mieg, J., Kim, J.K. (2009). 26G endo-siRNAs regulate spermatogenic and zygotic gene expression in Caenorhabditis elegans. PNAS 106, 18674–18679.

Heestand, B., Simon, M., Frenk, S., Titov, D., and Ahmed, S. (2018). Transgenerational Sterility of Piwi Mutants Represents a Dynamic Form of Adult Reproductive Diapause. Cell Rep. 23, 156–171.

Horwich, M.D., Li, C., Matranga, C., Vagin, V., Farley, G., Wang, P., and Zamore, P.D. (2007). The Drosophila RNA methyltransferase, DmHen1, modifies germline piRNAs and single-stranded siRNAs in RISC. Curr. Biol. 17, 1265– 1272.

Hulsen, T., de Vlieg, J., and Alkema, W. (2008). BioVenn—a web application for the comparison and visualization of biological lists using area-proportional Venn diagrams. BMC Genomics 9, 488.

Huntzinger, E., and Izaurralde, E. (2011). Gene silencing by microRNAs: contributions of translational repression and mRNA decay. Nat. Rev. Genet. 12, 99–110.

Iwasaki, Y.W., Siomi, M.C., and Siomi, H. (2015). PIWI-Interacting RNA: Its biogenesis and functions. Annu. Rev. Biochem. 84, 405–433.

Izumi, N., Shoji, S., Suzuki, Y., Katsuma, S., Tomari, Y. (2020). Zucchini consensus motifs determine the mechanism of pre-piRNA production. Nature 578, 311-316.

Jurka, J. (2000). Repbase update: a database and an electronic journal of repetitive elements. Trends Genet. 16, 418–420.

Kamath, R.S., Fraser, A.G., Dong, Y., Poulin, G., Durbin, R., Gotta, M., Kanapin, A., Le Bot, N., Moreno, S., Sohrmann, M., et al. (2003). Systematic functional analysis of the Caenorhabditis elegans genome using RNAi. Nature 421, 231–237.

Kamminga, L.M., van Wolfswinkel, J.C., Luteijn, M.J., Kaaij, L.J., Bagijn, M.P., Sapetschnig, A., Miska, E.A., Berezikov, E., and Ketting, R.F. (2012). Differential impact of the HEN1 homolog HENN-1 on 21U and 26G RNAs in the germline of Caenorhabditis elegans. PLoS Genet. 8, e1002702.

Kawamata, T., and Tomari, Y. (2010). Making RISC. Trends Biochem. Sci. 35, 368–376.

Ketting, R.F. (2011). The many faces of RNAi. Dev. Cell 20, 148–161.

Kim, K.W., Tang, N.H., Andrusiak, M.G., Wu, Z., Chisholm, A.D., and Jin, Y. (2018). A Neuronal piRNA Pathway Inhibits Axon Regeneration in *C. elegans*. Neuron 97, 511–519.e6.

Kuhn C.D., Joshua-Tor L. (2013). Eukaryotic Argonautes come into focus. Trends in Biochemical Sciences 38, 263-271.

Kurth, H.M., and Mochizuki, K. (2009). 20 -O-methylation stabilizes Piwi-associated small RNAs and ensures DNA elimination in Tetrahymena. RNA 15, 675–685.

Kwak J.E., and Wickens M. (2007). A family of poly(U) polymerases. RNA 13, 860-867.

Langmead, B. (2010). Aligning short sequencing reads with Bowtie. Curr. Protoc. Bioinformatics Chapter 11, Unit 11.17.

Lee, H.C., Gu, W., Shirayama, M., Youngman, E., Conte, D., Jr., and Mello, C.C. (2012). *C. elegans* piRNAs mediate the genome-wide surveillance of germline transcripts. Cell 150, 78–87.

Lee R.C., Feinbaum R.L., Ambros V., (1993) The *C. elegans* heterochronic gene lin-4 encodes small RNAs with antisense complementarity to lin-14. Cell 75: 843-854

Lee, Y., Kim, M., Han, J., Yeom, K.H., Lee, S., Baek, S.H., and Kim, V.N. (2004). MicroRNA genes are transcribed by RNA polymerase II. EMBO J. 23, 4051–4060.

Li, B., and Dewey, C.N. (2011). RSEM: accurate transcript quantification from RNA-Seq data with or without a reference genome. BMC Bioinformatics 12, 323.

Li, J., Yang, Z., Yu, B., Liu, J., and Chen, X. (2005). Methylation protects miRNAs and siRNAs from a 30 -end uridylation activity in Arabidopsis. Curr. Biol. 15, 1501–1507.

Livak, K.J., and Schmittgen, T.D. (2001). Analysis of relative gene expression data using real-time quantitative PCR and the 2(-Delta Delta C(T)) Method. Methods 25, 402–408.

Love, M.I., Huber, W., and Anders, S. (2014). Moderated estimation of fold change and dispersion for RNA-seq data with DESeq2. Genome Biol. 15, 550.

Luteijn, M.J., van Bergeijk, P., Kaaij, L.J., Almeida, M.V., Roovers, E.F., Berezikov, E., and Ketting, R.F. (2012). Extremely stable Piwi-induced gene silencing in Caenorhabditis elegans. EMBO J. 31, 3422–3430.

McMurchy, A.N., Stempor, P., Gaarenstroom, T., Wysolmerski, B., Dong, Y., Aussianikava, D., Appert, A., Huang, N., Kolasinska-Zwierz, P., Sapetschnig, A., et al. (2017). A team of heterochromatin factors collaborates with small RNA pathways to combat repetitive elements and germline stress. eLife 6, e21666.

Mello C.C., and Conte D. (2004). Revealing the world of RNA interference. Nature 431, 338-342.

Modepalli, V., Fridrich, A., Agron, M., and Moran, Y. (2018). The methyltransferase HEN1 is required in Nematostella vectensis for microRNA and piRNA stability as well as larval metamorphosis. PLoS Genet. 14, e1007590.

Montgomery, T.A., Rim, Y.S., Zhang, C., Dowen, R.H., Phillips, C.M., Fischer, S.E., and Ruvkun, G. (2012). PIWI associated siRNAs and piRNAs specifically require the Caenorhabditis elegans HEN1 ortholog henn-1. PLoS Genet. 8, e1002616.

Munafo, D.B., and Robb, G.B. (2010). Optimization of enzymatic reaction conditions for generating representative pools of cDNA from small RNA. RNA 16, 2537–2552.

Ouyang, J.P.T., Folkmann, A., Bernard, L., Lee, C.Y., Seroussi, U., Charlesworth, A.G., Claycomb, J.M., Seydoux, G. (2019). P granules protect RNA interference genes from silencing by piRNAs. Dev. Cell 50, 716-728.

Ozata, D.M., Gainetdinov, I., Zoch, A., O'Carroll, D., and Zamore, P.D. (2019). PIWI-interacting RNAs: small RNAs with big functions. Nat. Rev. Genet. 20, 89–108.

Pak, J., and Fire, A. (2007). Distinct populations of primary and secondary effectors during RNAi in *C. elegans*. Science 315, 241–244.

Pazdernik, N., and Schedl, T. (2013). Introduction to germ cell development in Caenorhabditis elegans. Adv. Exp. Med. Biol. 757, 1–16.

Phillips, C.M., Montgomery, T.A., Breen, P.C., and Ruvkun, G. (2012). MUT-16 promotes formation of perinuclear mutator foci required for RNA silencing in the *C. elegans* germline. Genes Dev. 26, 1433–1444.

Phillips, C.M., Brown, K.C., Montgomery, B.E., Ruvkun, G., and Montgomery, T.A. (2015). piRNAs and piRNA-Dependent siRNAs Protect Conserved and Essential *C. elegans* Genes from Misrouting into the RNAi Pathway. Dev. Cell 34, 457–465.

Pitt, J.N., Schisa, J.A., and Priess, J.R. (2000). P granules in the germ cells of Caenorhabditis elegans adults are associated with clusters of nuclear pores and contain RNA. Dev. Biol. 219, 315-333.

Reed, K.J., Svendsen, J.M., Brown, K.C., Montgomery, B.E., Marks, T.N., Vijayasarathy, T., Parker, D.M., Osborne Nishimura, E., Updike, D.L., Montgomery, T.A. (2020). Widespread roles for piRNAs and WAGO-class siRNAs in shaping the germline transcriptome of *Caenorhabditis elegans*. Nucleic Acids Research 48, 1811-1827.

Remmelzwaal, S., Boxem, M. (2019). Protein interactome mapping in *Caenorhabditis elegans*. Current Opinion in Systems Biology 13, 1-9

Ruby, J.G., Jan, C., Player, C., Axtell, M.J., Lee, W., Nusbaum, C., Ge, H., and Bartel, D.P. (2006). Large-scale sequencing reveals 21U-RNAs and additional microRNAs and endogenous siRNAs in *C. elegans*. Cell 127, 1193–1207.

Saito, K., Sakaguchi, Y., Suzuki, T., Suzuki, T., Siomi, H., and Siomi, M.C. (2007). Pimet, the Drosophila homolog of HEN1, mediates 2'-O-methylation of Piwi-interacting RNAs at their 3' ends. Genes Dev. 21, 1603–1608.

Sakaguchi, A., Sarkies, P., Simon, M., Doebley, A.L., Goldstein, L.D., Hedges, A., Ikegami, K., Alvares, S.M., Yang, L., LaRocque, J.R., et al. (2014). Caenorhabditis elegans RSD-2 and RSD-6 promote germ cell immortality by maintaining small interfering RNA populations. Proc. Natl. Acad. Sci. USA 111, E4323–E4331.

Seitz, H., Ghildiyal, M., and Zamore, P.D. (2008). Argonaute loading improves the 5' precision of both MicroRNAs and their miRNA* strands in flies. Curr. Biol. 18, 147–151.

Seth, M., Shirayama, M., Gu, W., Ishidate, T., Conte, D., Jr., and Mello, C.C. (2013). The *C. elegans* CSR-1 Argonaute Pathway Counteracts Epigenetic Silencing to Promote Germline Gene Expression. Dev. Cell 27, 656–663.

Seth, M., Shirayama, M., Tang, W., Shen, E.Z., Tu, S., Lee, H.C., Weng, Z., and Mello, C.C. (2018). The coding regions of germline mRNAs confer sensitivity to argonaute regulation in *C. elegans*. Cell Rep. 22, 2254–2264.

Seydoux, G. (2018). The P Granules of *C. elegans*: A Genetic Model for the Study of RNA-Protein Condensates. J. Mol. Biol. 430, 4702–4710.

Shen, E.Z., Chen, H., Ozturk, A.R., Tu, S., Shirayama, M., Tang, W., Ding, Y.H., Dai, S.Y., Weng, Z., and Mello, C.C. (2018). Identification of piRNA Binding Sites Reveals the Argonaute Regulatory Landscape of the *C. elegans* Germline. Cell 172, 937–951.e918.

Shirayama, M., Seth, M., Lee, H.C., Gu, W., Ishidate, T., Conte, D., Jr., and Mello, C.C. (2012). piRNAs initiate an epigenetic memory of nonself RNA in the *C. elegans* germline. Cell 150, 65–77.

Sijen, T., Steiner, F.A., Thijssen, K.L., and Plasterk, R.H. (2007). Secondary siRNAs result from unprimed RNA synthesis and form a distinct class. Science 315, 244–247.

Simon, M., Sarkies, P., Ikegami, K., Doebley, A.L., Goldstein, L.D., Mitchell, J., Sakaguchi, A., Miska, E.A., and Ahmed, S. (2014). Reduced insulin/IGF-1 signaling restores germ cell immortality to Caenorhabditis elegans Piwi mutants. Cell Rep. 7, 762–773.

Tabara, H., Yigit, E., Siomi, H., and Mello, C.C. (2002). The dsRNA binding protein RDE-4 interacts with RDE-1, DCR-1, and a DExH-box helicase to direct RNAi in *C. elegans*. Cell 109, 861–871.

Tang, W., Seth, M., Tu, S., Shen, E.Z., Li, Q., Shirayama, M., Weng, Z., and Mello, C.C. (2018). A sex chromosome piRNA promotes robust dosage compensation and sex determination in *C. elegans*. Dev. Cell 44, 762–770.

Thomson, T., and Lin, H. (2009). The biogenesis and function of PIWI proteins and piRNAs: progress and prospect. Annu. Rev. Cell Dev. Biol. 25, 355–376.

Thorvaldsdottir, H., Robinson, J.T., and Mesirov, J.P. (2013). Integrative Genomics Viewer (IGV): high-performance genomics data visualization and exploration. Brief. Bioinform. 14, 178–192.

Tolia, N.H., and Joshua-Tor, L. (2007). Slicer and the Argonautes. Nature Chemical Biology 3, 36.

Tomari, Y., and Zamore, P.D. (2005). Perspective: machines for RNAi. Genes and Dev. 19, 517-529.

Vasale, J.J., Gu, W., Thivierge, C., Batista, P.J., Claycomb, J.M., Youngman, E.M.,

Duchaine, T.F., Mello, C.C., and Conte, D., Jr. (2010). Sequential rounds of RNA-dependent RNA transcription drive endogenous small-RNA biogenesis in the ERGO-1/Argonaute pathway. Proc. Natl. Acad. Sci. USA 107, 3582–3587.

Wan, G., Fields, B.D., Spracklin, G., Shukla, A., Phillips, C.M., and Kennedy, S. (2018). Spatiotemporal regulation of liquid-like condensates in epigenetic inheritance. Nature 557, 679–683.

Wang, X., Wang, Y., Dou, Y., Chen, L., Wang, J., Jiang, N., Guo, C., Yao, Q., Wang, C., Liu, L., et al. (2018). Degradation of unmethylated miRNA/miRNA*s by a DEDDy-type 3' to 5' exoribonuclease Atrimmer 2 in Arabidopsis. Proc. Natl. Acad. Sci. USA 115, E6659–E6667.

Warf, M.B., Shepherd, B.A., Johnson, W.E., and Bass, B.L. (2012). Effects of ADARs on small RNA processing pathways in *C. elegans*. Genome Res. 22, 1488–1498.

Wedeles, C.J., Wu, M.Z., and Claycomb, J.M. (2013). Protection of Germline Gene Expression by the *C. elegans* Argonaute CSR-1. Dev. Cell 27, 664–671.

Wee, L.M., Flores-Jasso, C.F., Salomon, W.E., and Zamore, P.D. (2012). Argonaute divides its RNA guide into domains with distinct functions and RNA-binding properties. Cell 151, 1055-1067.

Wightman, B., Ha, I., and Ruvkun, G. (1993). Posttranscriptional regulation of the heterochronic gene lin-14 by lin-4 mediates temporal pattern formation in *C. elegans*. Cell 75, 855–862.

Winston, W.M., Molodowitch, C., and Hunter, C.P. (2002). Systemic RNAi in *C. elegans* requires the putative transmembrane protein SID-1. Science 295, 2456–2459.

Wu, W.S., Brown, J.S., Chen, T.T., Chu, Y.H., Huang, W.C., Tu, S., and Lee, H.C. (2019). piRTarBase: a database of piRNA targeting sites and their roles in gene regulation. Nucleic Acids Res. 47, D181–D187.

Xu, F., Feng, X., Chen, X., Weng, C., Yan, Q., Xu, T., Hong, M., and Guang, S. (2018). A Cytoplasmic Argonaute Protein Promotes the Inheritance of RNAi. Cell Rep. 23, 2482–2494.

Yang, H., Zhang, Y., Vallandingham, J., Li, H., Florens, L., and Mak, H.Y. (2012). The RDE-10/RDE-11 complex triggers RNAi-induced mRNA degradation by association with target mRNA in *C. elegans*. Genes Dev. 26, 846–856.

Yigit, E., Batista, P.J., Bei, Y., Pang, K.M., Chen, C.C., Tolia, N.H., Joshua-Tor, L., Mitani, S., Simard, M.J., and Mello, C.C. (2006). Analysis of the *C. elegans* Argonaute family reveals that distinct Argonautes act sequentially during RNAi. Cell 127, 747–757.

Yu, B., and Chen, X. (2010). Analysis of miRNA Modifications. Methods Mol. Biol. 592, 137–148. Yu, B., Yang, Z., Li, J., Minakhina, S., Yang, M., Padgett, R.W., Steward, R., and Chen, X. (2005). Methylation as a crucial step in plant microRNA biogenesis. Science 307, 932–935.

Zhang, C., Montgomery, T.A., Gabel, H.W., Fischer, S.E., Phillips, C.M., Fahlgren, N., Sullivan, C.M., Carrington, J.C., and Ruvkun, G. (2011). mut-16 and other mutator class genes modulate 22G and 26G siRNA pathways in Caenorhabditis elegans. Proc. Natl. Acad. Sci. USA 108, 1201–1208.

Zhang, C., Montgomery, T.A., Fischer, S.E., Garcia, S.M., Riedel, C.G., Fahlgren, N., Sullivan, C.M., Carrington, J.C., and Ruvkun, G. (2012). The Caenorhabditis elegans RDE-10/RDE-11 complex regulates RNAi by promoting secondary siRNA amplification. Curr. Biol. 22, 881–890.

Zhang, D., Tu, S., Stubna, M., Wu, W.S., Huang, W.C., Weng, Z., and Lee, H.C. (2018). The piRNA targeting rules and the resistance to piRNA silencing in endogenous genes. Science 359, 587–592.

APPENDIX 1: Supplementary Material for Chapter 2

The sequencing data for this study were published under the GEO accession number GSE137734. Supplementary tables have been uploaded alongside this dissertation in the form of Excel spreadsheets.

Supplementary data for chapter 2 can also be found online at https://www.cell.com/cell-reports/fulltext/S2211-1247(19)31447-0#secsectitle0210

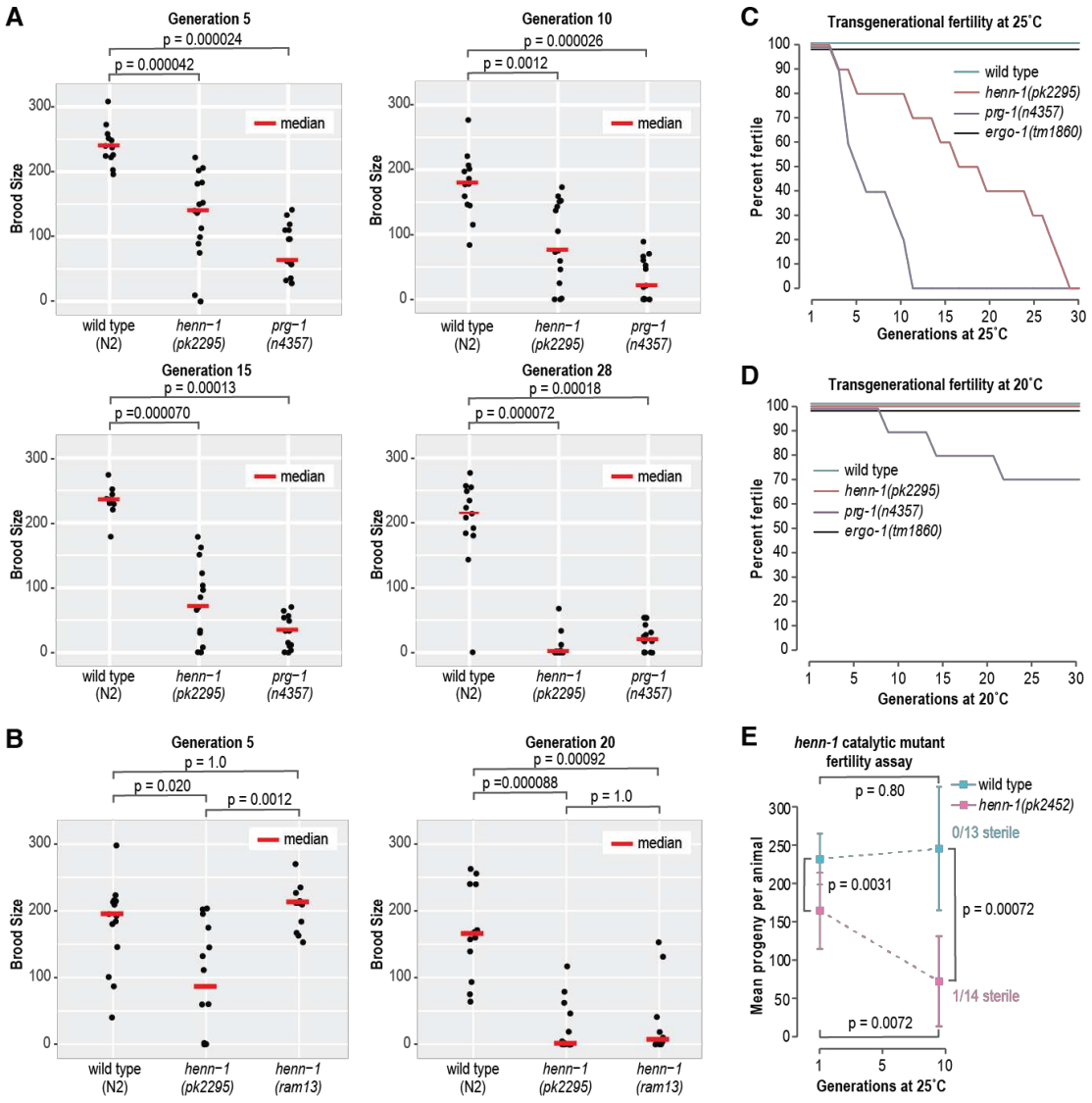

Figure S1. Related to Figure 1. *henn-1* transgenerational fertility assays. (A) Brood sizes of wild type, henn1*(pk2295)*, and *prg-1(n4357)* at ~5, ~10, ~15, and ~28 generations. Bonferroni adjusted p values were calculated using Wilcoxon rank-sum tests. Each data point represents the number of progeny produced by one animal. Results summarized in Figure 1A. (B) Brood sizes of wild type, *henn-1(pk2295)*, and *henn-1(ram13)* at ~5 and ~20 generations. Bonferroni adjusted p values calculated using Wilcoxon rank-sum tests. Results summarized in Figure 1B. (C-D) Percentages of 10 independent lines of wild type, *henn-1(pk2295)*, prg1*(n4357)*, and *ergo-1(tm1860)* that remained fertile at each generation at 25˚C (C) and 20˚C (D). Animals that produced any progeny were considered fertile. (E) Brood sizes of wild type and *henn-1*(pk2452) (catalytic domain mutant) at 1 generation (wild type, n = 15; *henn-1*, n = 13)

and 10 generations (wild type, n = 13; henn1, n = 14) at 25˚C. The numbers of sterile animals at 10 generations are shown. Bonferroni adjusted p values were calculated using Wilcoxon rank-sum tests.

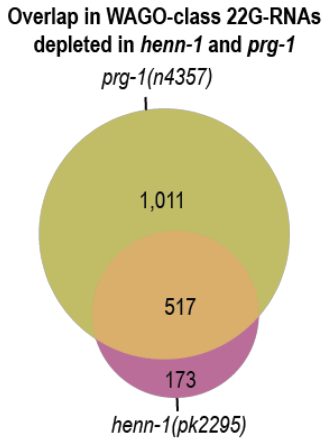

Figure S2. Related to Figure 2. Most *henn-1*-dependent 22G-RNAs are derived from piRNA targets. The Venn diagram displays overlap in WAGO-class 22G-RNAs that are depleted >50% in *henn-1(pk2295)* and prg1*(n4357)* adult whole animals relative to wild type.

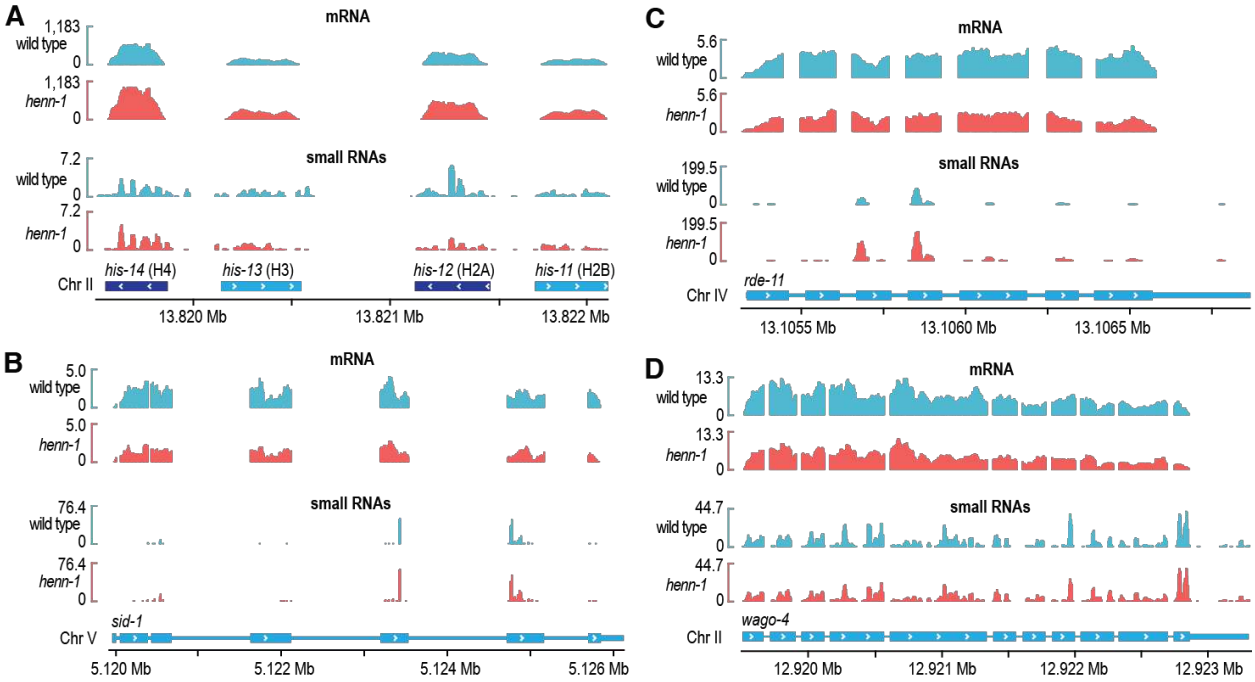

Figure S3. Related to Figure 3. Small RNA and mRNA misregulation in *henn-1* mutants. (A) mRNA and small RNA read distribution across a histone cluster in wild type and *henn-1(pk2295)*. (B) mRNA and small RNA read distribution across sid-1 in wild type and *henn-1(pk2295)*. (C) mRNA and small RNA read distribution across *rde-11* in wild type and *henn-1(pk2295)*. (D) mRNA and small RNA read distribution across wago-4 in wild type and *henn-1(pk2295)*. Plots were generated in IGV.

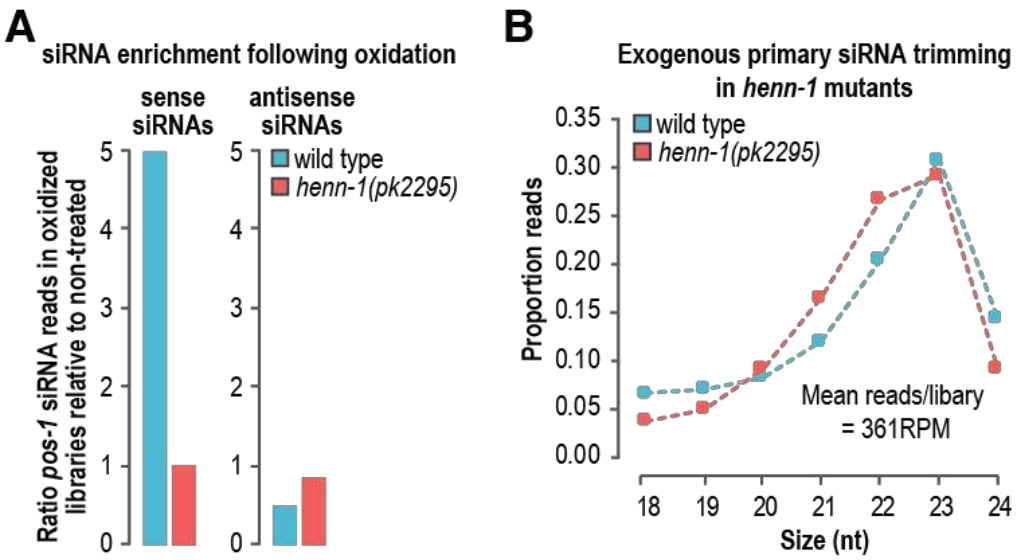

Figure S4. Related to Figure 4. *henn-1* is required for primary siRNA methylation. Bar plots display the ratio of normalized reads mapping to pos-1 in sodium periodate treated (oxidation +) and control treated (oxidation -) wild type and *henn-1(pk2295)* small RNA libraries. The left plot includes only sense-mapping reads to pos-1, which are presumably primary siRNAs. The right plot includes only antisense siRNAs, which are predominantly secondary siRNAs (22G-RNAs).

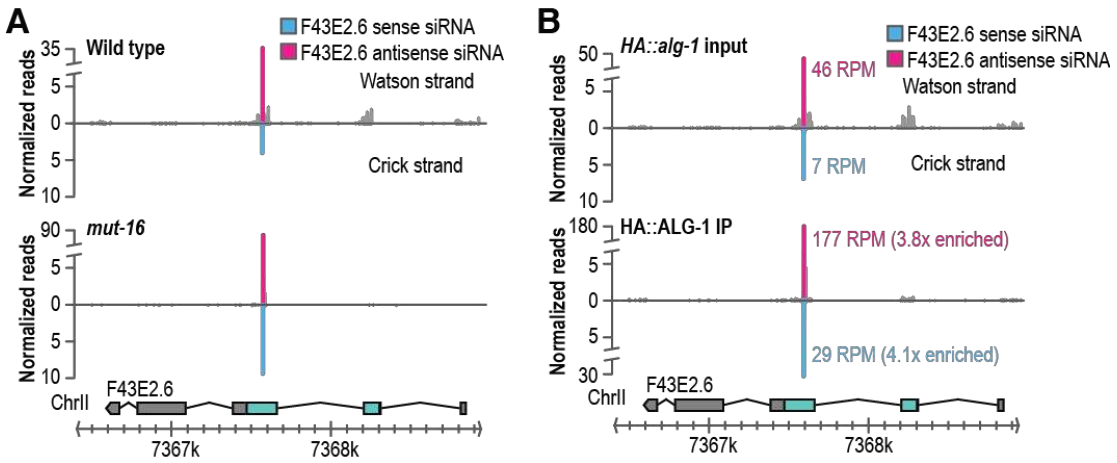

Figure S5. Related to Figure 5. F43E2.6 is a mut-16-independent siRNA locus. (A) Normalized read distribution across the F43E2.6 siRNA-generating locus in wild type (upper panel) and mut-16(pk710) (lower panel). Sense siRNA reads are in blue and antisense are in magenta. (B) Normalized read distribution (reads per million total, RPM) across the F43E2.6 siRNA-generating locus from HA::alg-1 cell lysate (upper panel) and HA::ALG-1 co-IP (lower panel). Fold enrichment in HA::ALG-1 co-IP relative to cell lysate is shown.

APPENDIX 2: Attempts to Characterize the Small RNA Decay Machinery

This appendix describes experiments directed at identifying the small RNA decay machinery in *C. elegans*. Although none of them conclusively identified any participants in the small RNA turnover pathway, they provide a starting point from which this question may be approached in the future.

3' methylation is typically a protective measure against small RNA degradation, and the specific machinery that degrades small RNAs in *C. elegans* remains unknown. To identify potential degradation factors, we developed an RNAi-based genetic screen. The screen was designed to take advantage of the sterility expressed by worms in which RNAi has been reset in the absence of methylated piRNAs, as this sterility is presumably due to piRNA destabilization in methylation mutants (see Figure A1 as well as Figure 2.1 C-E and associated text for more information). By performing feeding RNAi against potential genes of interest during this RNAi reset cross, we hoped to identify genes that degrade unmethylated piRNAs by knocking them down so that they can no longer perform small RNA turnover. Any gene that restored fertility would be considered a gene of interest and would be further investigated for roles in piRNA decay. Since disabling the secondary siRNA biogenesis pathway also restores fertility during RNAi reset, RNAi against *mut-2*, a gene essential for secondary siRNA formation, was used as a positive control (Figure A1).

In other organisms, small RNA degradation is preceded by polyuridylation. Therefore, we first compiled a list of annotated and predicted exonucleases and poly(U) polymerases to screen (Tables A1 and A2). Among the tested genes, *pup-3*, an

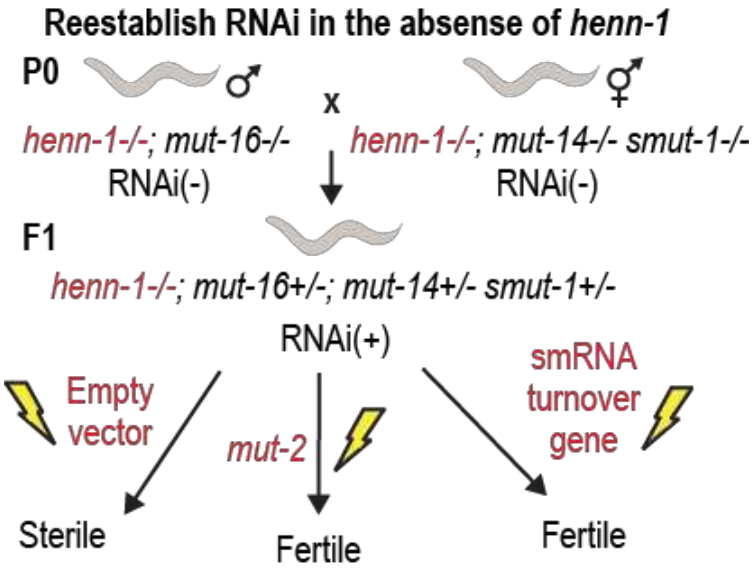

Figure A1. Resetting RNAi for genetic screening. A diagram demonstrating the expected outputs from the genetic screen used to identify potential small RNA turnover genes under each of the indicated RNAi treatments.

annotated poly(U) polymerase with no known function (Kwak and Wickens, 2007), emerged from the screen as a potential participant in the piRNA turnover pathway. Although it failed to reproduce its robust suppression of sterility during repeated trials, it was nonetheless deemed promising enough to carry forward for closer analysis. *pup-3(tm5089)* was crossed into *henn-1(pk2295)*, and this double mutant was crossed into either *mut-16(pk710)* or *mut-14(mg464);smut-1(tm1301)* to perform the RNAi reset cross with the addition of the *pup-3* mutation. As in the RNAi screen, *henn-1;pup-3* double mutants were not statistically significantly more fertile than mutants for *henn-1* (Figure A2A). Alongside this experiment, we used TaqMan qPCR to measure the abundance of several piRNAs (all of which have been previously shown to be methylation dependent by Montgomery et al., 2012) at two developmental stages: L1s and L4s. In addition to these piRNAs, we examined an ERGO-1-class 26G RNA at the L4 stage to measure the effect, if any, of *pup-3* on another class of methylated small RNA and a Mutator-dependent secondary siRNA at the L1 stage to measure the effect, if any, of *pup-3* on the downstream RNAi pathway. In both L1s (Figure A2B) and L4s (Figure A2C), *pup-3* mutation failed to rescue the small RNA depletion associated with loss of *henn-1*. In all cases, *henn-1* mutants were indistinguishable from *henn-1;pup-3* double mutants.

In addition to examining poly(U) polymerases, we asked whether the RNA-modifying enzymes of the Mutator complex degrade unmethylated small RNAs. To test this, we generated *mut-16(pk710);henn-1(pk2295)* double mutants that are deficient for both primary small RNA methylation and secondary small RNA production. We then tested the abundance of piRNAs in these mutants. Compared to wild type, *henn-1(pk2295)*

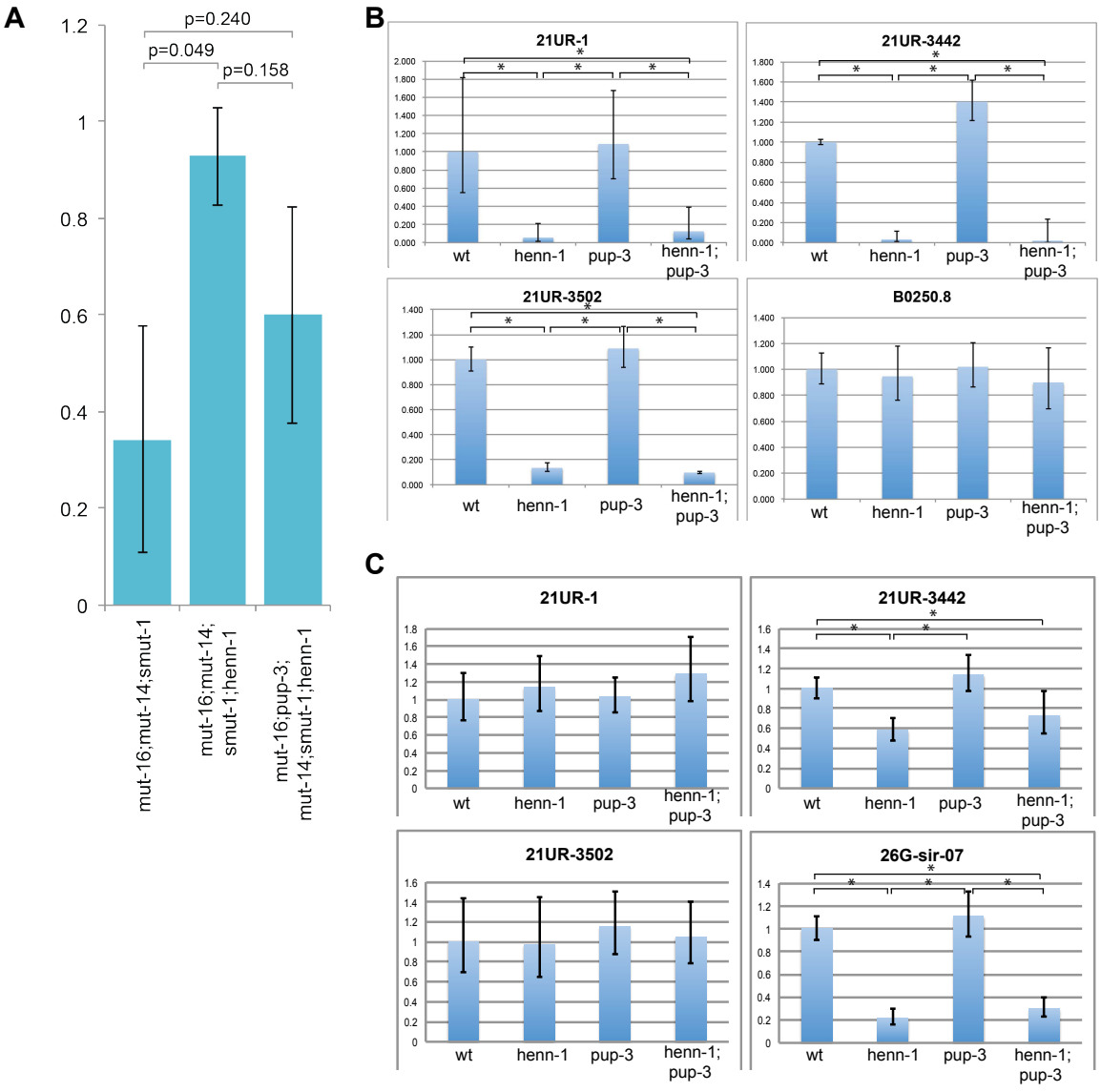

Figure A2. *pup-3*'s influence on fertility and small RNA abundance.
(A) Fertility after resetting RNAi in the presence and absence of *henn-1* and *pup-3*. Results represent 3 crosses in *mut-16(pk710);mut-14(mg464);smut-1(tm1301)* (19 total offspring scored), 2 crosses in *mut-16(pk710);mut-14(mg464);smut-1(tm1301);henn-1(pk2295)* (13 total offspring scored), and 3 crosses in *mut-16(pk710);pup-3(tm5089);mut-14(mg464);smut-1(tm1301);henn-1(pk2295)* (24 total offspring scored). (B) Abundance of each of the indicated piRNAs (21UR-1, 21UR-3442, 21UR-3502) and a secondary siRNA derived from the B0250.8 locus in L1s measured by TaqMan qPCR. Comparisons marked with an asterisk are statistically significant ($p < 0.05$, Student's t-test), all other comparisons are nonsignificant. (C) Abundance of each of the indicated piRNAs (21UR-1, 21UR-3442, 21UR-3502) and the ERGO-1-class 26G-RNA 26G-siR-07 in L4s measured by TaqMan qPCR. Comparisons marked with an asterisk are statistically significant ($p < 0.05$, Student's t-test), all other comparisons are nonsignificant.

mutants displayed an increase in piRNA reads, likely due to the decreased efficiency of ligating the 3' adapter to small RNAs that are methylated on the 3' end. Also consistent with a loss of methylation, *henn-1* mutants showed an increase in the proportion of truncated piRNAs (Figure A3). When compared to *henn-1* single mutants, *mut-16(pk710);henn-1(pk2295)* double mutants were expected to show a decrease in truncated piRNAs, as the interaction between the unmethylated small RNAs and the Mutator proteins was expected to decrease. Instead, we saw an increase in the proportion of trimmed piRNAs in the double mutants (Figure A3).

Although the result of this experiment suggests that the mutator complex does not contribute to degrading unmethylated small RNAs, it has two substantial caveats that should be considered while interpreting the results. First, this experiment represents only one biological replicate that was submitted for sequencing, so these results could be considered suggestive, but by no means definitive. Second, although the *mut-16* mutation that we introduced abolishes secondary siRNA formation, it likely does so because it prevents the Mutator complex from nucleating. This means that its constituent proteins could still be functional and may be able to act on unmethylated small RNAs with the same frequency as *mut-16* wild type animals. Future efforts to examine the Mutator proteins' contributions to the turnover of unmethylated small RNAs could circumvent this issue by directly mutating *mut-7,* a known exonuclease in the Mutator complex. Due to *mut-7*'s proximity to *henn-1* on chromosome III, however, it would be necessary to use non-traditional genetic methods such as CRISPR Cas9 to introduce this mutation.

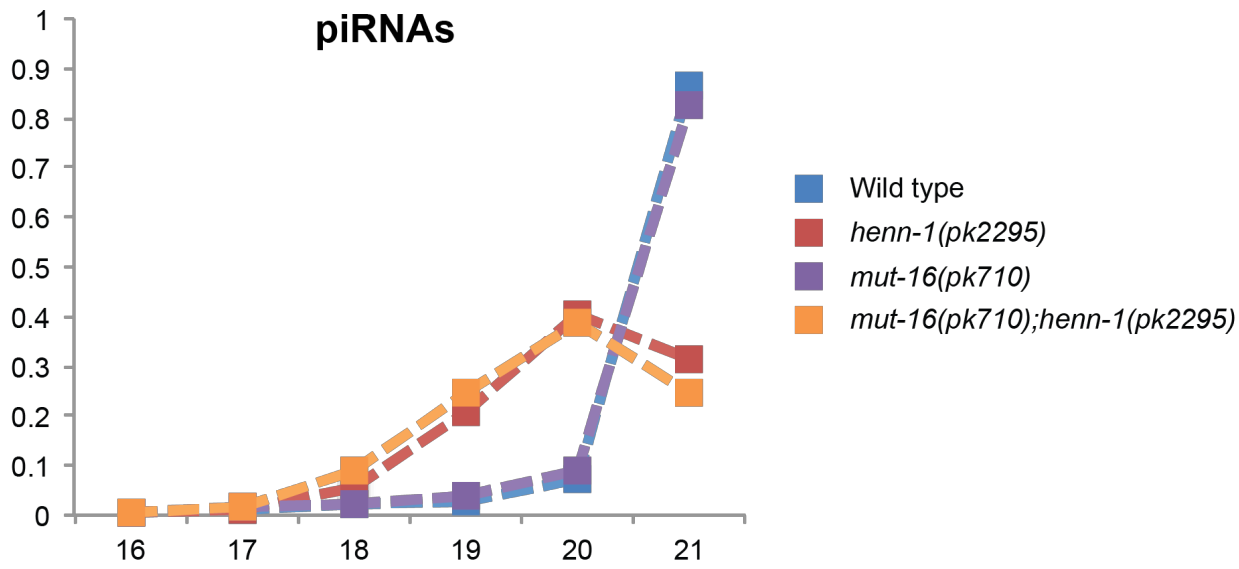

Figure A3. Length of piRNAs in methylation and Mutator mutants.
The proportions of total high-throughput sequencing reads for piRNAs in each of the indicated strains plotted by size. The piRNA reads per million total reads in each library are as follows: 69.6 kRPM for wild type, 281.6 kRPM for *henn-1*, 67.2 kRPM for *mut-16*, and 272.2 kRPM for *mut-16;henn-1*.

Since it is possible that *pup-3* acts in tandem with another redundant or partially redundant poly(U) polymerase as is the case in *Arabidopsis*, we identified other genes of similar function to investigate alongside *pup-3* in future experiments. In this case, we examined *cde-1* (also known as *cid-1* or *pup-1*) and *pup-2*. While *pup-3* mutation appeared to have little measurable effect on worm health alone, both *cde-1* and *pup-2* mutants were unhealthy and highly susceptible to temperature-dependent sterility when grown at 25C. Additionally, they were difficult to work with genetically, as *henn-1, cde-1,* and *pup-2* are all in relatively close proximity on chromosome III and generally failed to segregate during crosses. Finally, assessing their influence on fertility while resetting RNAi was difficult, as they would also need to be combined with mutants for Mutator genes *mut-16* and *mut-14;smut-1* in order to perform the experimental cross. These limitations ultimately resulted in the suspension of further investigation into these poly(U) polymerases in order to pursue more fruitful aspects of the larger effort to functionally characterize small RNA methylation, but any future efforts to examine small RNA turnover in *C. elegans* may find these genes to be worth consideration.

Finally, another screen was developed with the intent of increasing throughput by circumventing the need to reset RNAi for every gene that was tested. In this screen, fluorescent sensors for piRNA (*mex-5::mCherry-21ur2921as*) and secondary siRNA (*ubl-1-GFP-SiR-1-sensor;ubl-1-mCherry-SiR-1-sensor*) activity were introduced to *henn-1(pk2295)* mutants. Compared to animals in which the RNAi pathway is functional, these sensors are brighter in RNAi deficient animals. Compared to untreated *henn-1* mutants, those in which the RNAi treatment disabled the small RNA decay pathway were expected to resemble *henn-1* wild type animals more closely than *henn-1* mutants.

Although this screen did not produce any conclusive genes of interest, the use of fluorescent reporters should not be discounted. A screen employing a sufficiently sensitive sensor could conceivably be an efficient way to test large numbers of genes quickly. The sensors we used, however, were not capable of resolving differences between wild-type and mutant animals and, therefore, were unable to produce useful results.

Since the lists of genes we intended to screen included 19 poly(U) polymerases and 55 exonucleases (see Tables A1 and A2), it would be ideal to employ the simplest possible genetic screen to maximize throughput and efficiency. Unfortunately, it may be necessary to make use of other approaches that use readouts other than fertility and fluorescent reporters. One possibility is to use an approach like Tang et al. (2016) used to identify the *parn-1* as the exonuclease that trims piRNA precursors in *C. elegans.* They isolated RNA from animals undergoing RNAi treatment against candidate nucleases and subjected them to northern blotting to look for changes in piRNA length. Since northern blotting has previously shown piRNA truncations in *henn-1* mutants (Billi et al., 2012; Kamminga et al., 2012; Montgomery et al., 2012), it could also reveal loss of truncation in *henn-1* mutants undergoing knockdown of a nuclease that degrades unmethylated small RNAs. If we are correct that polyuridylation precedes degradation, it could presumably show a loss of piRNA decay during poly(U) polymerase knockdown as well. It would be a labor intensive and potentially hazardous approach, but it provides a readout that is hopefully clearer and more consistent than the screens we have attempted in the past.

Another, even more labor intensive approach would be to perform protein-protein crosslinking in *henn-1* mutants to attempt to identify proteins that interact with methylated small RNA-associated Argonautes when methylation is not there to protect the RNAs. Proteins found to interact with these Argonautes could be further investigated for roles in the decay pathway. Another option could be to crosslink proteins to RNA in *henn-1* mutants with the intent of identifying proteins in the process of tailing or degrading unmethylated piRNAs. Both of these approaches have in common the flaw that any proteins shown to interact in a way that suggests participation in the degradation pathway still need to be positively identified by other means. This means that, unlike some of the other proposed and attempted screen-based approaches, the identity of the gene contributing to the observed phenotype is not immediately known. There is also the issue that even if proteins interact more frequently with Argonautes or piRNAs in *henn-1* mutants, it wouldn't necessarily mean they are involved in the degradation process. Despite these caveats, crosslinking may be an overall useful, if inefficient, way to approach this question should other options fail.

It may also be possible to use proximity labeling systems to identify unknown proteins that interact with HENN-1 or methylation-directing Argonautes. Although such tools are used infrequently in *C. elegans* (Remmelzwaal and Boxem, 2019), the biotin ligase TurboID has been used to label proteins in live *C. elegans* embryos (Branon et al. 2018). Attaching TurboID to PRG-1, RDE-1, or ERGO-1 could allow for the enrichment of factors that interact with these argonautes in both the presence and absence of *henn-1*, potentially revealing the proteins that participate in small RNA degradation. Employing such a technique comes with many of the same caveats as protein

crosslinking along with the additional difficulty of being a method for which few resources exist in *C. elegans* research, but could ultimately prove to be the most effective way to identify the components of the small RNA turnover pathway. Although it is likely to be difficult, this pathway has not been characterized in any organism, and doing so would fill a long-standing gap in our understanding of small RNA biology.